Broadly Neutralizing Antibody Epitopes on HIV-1 Particles are exposed after Virus Interaction with Host Cells

Priyanka Gadam Rao[a], Gregory S. Lambert[a], and Chitra Upadhyay[a]*

[a]Division of Infectious Disease, Department of Medicine, Icahn School of Medicine at Mount Sinai, New York, New York, USA

Running Head: Unmasking epitopes for HIV-1 Neutralization

* Address correspondence to chitra.upadhyay@mssm.edu

Abstract Word Count: 249

Importance word count: 115

Text word count: 6795

Keywords: Human immunodeficiency virus; neutralization; antibodies; broadly neutralizing antibodies (bNAbs); non-neutralizing antibodies (nNAbs); envelope conformations.

Abstract

HIV-1 envelope glycoproteins (Env) are critical for infection and are key targets for vaccine development. Env proteins displayed on virions are conformationally diverse, comprising both functional and non-functional forms. These heterogeneous Env populations have important implications for neutralizing and non-neutralizing antibody elicitation and functions. This study aimed to interrogate the antigenic composition of Env on virions. Using a flow cytometry-based assay we show that only some epitopes including V2i, gp120-g41 interface, and gp41-MPER are accessible on HIV-1 particles, while V3, V2q, and select CD4bs epitopes are obscured for monoclonal antibody (mAb) binding. To investigate the mechanisms contributing to the masking of these epitopes we first asked whether time-dependent dynamics of Env can affect their exposure. Extending the time of virus-mAb interaction increased the binding of mAbs, epitopes of which were already accessible on virions but not those that are occluded. However, the occluded epitopes became accessible after conformational unmasking was induced by pre-binding of select mAbs, prompting us to test if similar conformational changes are required for these mAbs to exhibit their neutralization capability. We tested HIV-1 neutralization where virus-mAb mix was incubated or not incubated for one-hour prior to adding the target cells. Similar levels of neutralization were observed under both assay conditions, suggesting that interaction between virus and cells sensitizes the virions for neutralization via broadly-neutralizing antibodies (bNAbs). These findings provide insight into how bNAbs may gain access to these occluded epitopes to exert their neutralization effects. Further studies with larger virus and mAb panels are warranted.

Importance

The human immunodeficiency virus (HIV-1) envelope (Env) glycoprotein spike mediates viral entry, and is the sole target of neutralizing antibodies. Our data suggest that epitopes of broadly neutralizing antibodies (bNAbs) including the V2q (e.g., PG9, PGT145), CD4bs (e.g., VRC01, 3BNC117) and V3 (2219, 2557) are masked on the REJO, and CMU06 virus particles. The PG9 and 2219 epitopes became accessible after conformational unmasking was induced by pre-binding of select mAbs. Attempt to understand the masking mechanism led to the revelation that interaction between virus and cells is needed to sensitize the virions for neutralization via bNAbs. These findings provide insight into how bNAbs may gain access to these occluded epitopes to exert their neutralization effects.

1. Introduction

The envelope glycoprotein (Env) of Human immunodeficiency virus type-1 (HIV-1) is the virus attachment protein that interacts with the host-cell receptor CD4 and chemokine receptors CCR5 or CXCR4 to initiate infection (1). Env is the only viral protein on the surface of HIV-1 particles, and is therefore a sole target for HIV-1 broadly neutralizing antibodies (bnAbs) that neutralize the virus and prevent infection of host cells. Env exists as a trimer of gp120-gp41 heterodimers which remains noncovalently associated in a prefusion "closed" conformation that can dynamically sample alternative conformational states. (2-9). These conformations are extremely important and are involved in the infection process and also in Env's interaction with host mounted antibodies (Abs) (4, 10-13). The gp120 subunit comprises five variable (V1-V5) and five conserved (C1-C5) regions, with the V1V2 from each protomers joining at the top to form the trimer apex, a immunogenic structurally conserved region targeted by some of the most potent HIV-1 bNAbs (14-18). The gp41 comprises the fusion machinery, mediating entry of the virus into the target cell by facilitating membrane fusion (19, 20).

HIV-1 displays an average of 7-14 Env trimers per particle. However, this number varies among isolates (21). HIV-1 Env is synthesized as a gp160 precursor protein in the endoplasmic reticulum (ER), where signal peptide cleavage, folding, addition of high-mannose glycans and trimerization in association with molecular chaperones takes place (22-25). Once the nascent polypeptide attains its native folding state, the Env egresses from the ER and translocates to the Golgi apparatus (26-33). In the Golgi, gp160 is cleaved by host furin-like proteases to generate a transmembrane gp41 subunit and non-covalently associated surface gp120 subunit. Three gp120-gp41 heterodimers assemble to form the

trimeric functional Env spikes that are then directed to the plasma membrane for incorporation into the virions (30-33). While trimeric Env is expected to be the most abundant form of Env present on virions, non-functional Env such as dimers, monomers, and gp41 stumps may also be present (34-36). These nonfunctional Env forms serve as decoys to divert the immune response away from vulnerable conserved epitopes, and also impart the diversity among the different Env forms on virions. Thus, HIV-1 particles may carry both functional and non-functional Env forms. An additional layer of diversity is afforded by the N-linked glycans that decorate the Env (37). These glycans comprise half of Env's molecular mass and play a critical role in cloaking the vulnerable Env epitopes. Thus, the population of Env that is encountered by the host immune system is highly heterogeneous.

Several monoclonal antibodies (mAbs) have been isolated from HIV-1 infected individuals and also from vaccinees from clinical trials that have helped to identify and map the vulnerable Env epitopes. These mAbs are categorized into distinct types based on their neutralization breadth and potency. The antibodies that potently neutralize multiple HIV-1 strains are referred as bNAbs and are unique in that they target conserved epitopes of the virus, meaning the virus may mutate, but the targeted epitopes will still exist. The weak- or non-neutralizing antibodies (wNAbs, nNAbs) bind to the Env in a manner that is not efficient at blocking virus infection. The bNAbs known to date have been isolated from HIV-1 infected individuals, and elicitation of these kind of mAbs via vaccination has not yet been achieved. In contrast, nNAbs or wNAbs including those that target the V1V2 and V3 regions, are readily elicited via various Env vaccines as well as during HIV-1 infection (38-47). The HIV-1 antibodies are further categorized based on the distinct Env region that

they target such as V1V2, V3, CD4bs, gp41-MPER, and the gp120-gp41 interface (48). While most mAbs are conformation-dependent some also recognize linear epitopes. For example, the V1V2 mAbs are categorized into three types (V2i, V2p and V2q) based on their binding mode (49, 50). V2i-specific mAbs, (e.g., 697, 830A and 2158) recognize V1V2 when its V2C region is in a β-strand configuration; the epitope region of these V2i mAbs is discontinuous, highly conformational, and overlaps the α4β7 integrin-binding motif (49). The V2p mAbs, (eg., CH58 and CH59) were isolated from RV144 vaccinees and target a linear peptide region on V2; these mAbs recognize V2 when the V2C strand region is in an α-helix and extended coil conformation (51-53). The epitope region recognized by V2q mAbs (e.g., PG9, PG16, and PGT145) includes two N-linked glycans (N156 and N160) and consists of the V2C in its β-strand configuration (15, 54-56). Another key distinction is whether the mAbs recognize Env in the context of functional trimers for e.g., PG9, PG16, and VRC01 (34, 57, 58). Binding of antibodies to their target epitopes on Env is essential for exerting the protective role either by virus neutralization or via their Fc-receptor effector functions (59, 60). The Env conformational diversity and the presence of the functional and non-functional Envs on virions can have a profound influence on antibody elicitation and function. However, it is unclear if distribution and accessibility of these various Env epitopes on virions is similar or varies between HIV-1 isolates from different clades or stages of infection.

In this study, we aimed to understand the overall antigenic makeup of the Env that is present at the surface of HIV-1 particles. We established a flow cytometry based assay to detect the binding of anti-HIV-1 mAbs targeting different Env regions and epitopes present on the virus particles. We then used our assay to compare the antigenic presentation

of virus-associated Env using HIV-1 isolates that are from different infectious stages, clades, and neutralization tiers. Using REJO (transmitted-founder (T/F); clade B, tier 2), CMU06 (acute; clade AE, tier 2) and SF162 (chronic; clade B, tier 1) viruses, we show that the epitopes accessible on virions are largely similar and only select mAbs can bind to the purified virus particles. This binding pattern was different when compared to the binding of the same mAbs to Env expressed on the cell surface. As expected, V3 epitopes were not accessible on virions and binding of V3 mAbs were comparable to the negative control anti-anthrax mAb 3685. Notably, bNAbs that target the quaternary epitopes at the trimer apex —PG9, PG16, and PGT145— were also unable to bind to their V1V2 epitopes on all three virus isolates tested. In order to neutralize HIV-1, it is essential that an antibody bind to its epitope on the virions. A standard neutralization assay requires pre-incubation of the virus and Ab for one hour prior to adding the target cells (61-63). Prolonging the virus-mAb interaction time for up to 75 minutes did not expose the masked V1V2 or V3 epitopes. However, allosteric alterations induced by pre-binding of select mAbs improved their exposure as measured by the binding of biotinylated PG9 and 2219 mAbs. This led us to investigate if similar conformational changes are induced upon binding of the virions to the host cells, allowing the bNAbs to latch onto their epitopes and exert the neutralization effect. Indeed, adding virus-bNAb mixture to the target cells without prior incubation produced similar level of neutralization compared to standard assay conditions where virus-bNAb mixtures are incubated for one hour prior to adding the cells. Here, we report for the first time that bNAbs such as PG9, PGT145, NIH45-46, VRC01 and 3BNC117 can neutralize tier 2 isolates REJO and CMU06 without the need for a pre-incubation step. Thus, a virus-mAb pre-incubation step that is followed widely in the field does not appear

to be required for neutralization by these bNAbs. These data suggest that virus interaction with target cells induced changes in Env that exposed the epitopes recognized by these bNAbs, allowing their binding and virus neutralization. These findings are relevant as under physiological conditions, virus, Abs, and cells all are present in the same milieu at the same time. Given that bNAbs are the ideal for providing sterilizing immunity and are the goal of current HIV-1 vaccine efforts these data offer insight on how HIV-1 may occlude these vulnerable epitopes from host immune response. Further studies to precisely clarify the HIV-1 entry and neutralization mechanism are warranted.

2. Materials and Methods

Cell lines: HEK293T/17 cells were obtained from the American Type Culture Collection (ATCC, Manassas, VA). The following reagent was obtained through the NIH HIV Reagent Program, Division of AIDS, NIAID, NIH: TZM-bl Cells, ARP-8129, contributed by Dr. John C. Kappes, Dr. Xiaoyun Wu and Tranzyme Inc. (64). For all experiments, HEK293T/17 cells (293T) were used to produce infectious HIV-1 viruses and the TZM.bl cell line was used to assay virus infectivity. TZM.bl cell line is derived from HeLa cells and is genetically modified to express high levels of CD4, CCR5 and CXCR4 and contains reporter cassettes of luciferase and β-galactosidase that are each expressed from an HIV-1 LTR. The 293T and TZM.bl cell lines were routinely sub-cultured every 3 to 4 days by trypsinization and were maintained in Dulbecco's Modified Eagle's Medium (DMEM) supplemented with 10% heat-inactivated fetal bovine serum (FBS), HEPES pH 7.4 (10 mM), L-glutamine (2 mM), penicillin (100 U/ml), and streptomycin (100 μg/ml) at 37°C in a humidified atmosphere with 5% CO2.

Plasmids: A full-length transmitted/founder (T/F) infectious molecular clone (IMC) of pREJO.c/2864 (REJO, ARP-11746) was obtained through the NIH HIV Reagent Program, Division of AIDS, NIAID, NIH, contributed by Dr. John Kappes and Dr. Christina Ochsenbauer (65). REJO is a tier 2, clade B, T/F isolate. IMCs of SF162 (chronic; clade B, chronic, tier 1B) and CMU06 (acute; clade AE, acute, tier 2) were generated by cloning the Env into pNL4.3 backbone to construct pNL-CMU06 and pNL-SF162, respectively (66).

Antibodies: The following antibody reagents used in this study were obtained through the NIH AIDS Reagent Program, Division of AIDS, NIAID, NIH: Anti-HIV-1 gp120 monoclonal PG9, PG16, PGT145, PGT121, PGT128, from IAVI (67); anti-HIV-1 gp120 monoclonal CH59 from Drs. Barton F. Haynes and Hua-Xin Liao (52); anti-HIV-1 gp120 monoclonal VRC01 from Dr. John Mascola (68); anti-HIV-1 gp120 Monoclonal b12 from Dr. Dennis Burton and Carlos Barbas (69); anti-HIV-1 gp120 monoclonal 3BNC117 from Dr. Michel C. Nussenzweig (70); anti-HIV-1 gp120 monoclonal 17b from Dr. James E. Robinson (71); anti-HIV-1 gp41-gp120 monoclonal 35O22, from Drs. Jinghe Huang and Mark Connors (72); anti-HIV-1 gp41-gp120 monoclonal PGT151 from Dr. Dennis Burton; anti-HIV-1 gp41 monoclonal 2F5 and 4E10 from Polymun Scientific (73). The V2i and V3 mAbs were obtained from the laboratory of Dr. Susan Zolla-Pazner (74-81). An irrelevant anti-anthrax mAb 3685 (82) was used as a negative control.

Virus production and purification: Infectious viruses were generated by transfecting 293T cells with pREJO, pNL-SF162 and pNL-CMU06 plasmids using jetPEI transfection reagent (Polyplus, New York, NY) (83). Supernatants were harvested after 48 hours and clarified by centrifugation and 0.45μm filtration. Virus infectivity was assessed on TZM.bl

cells as described (83, 84). Briefly, serial two-fold dilutions of virus stock in 10% DMEM were incubated with TZM.bl cells (in duplicates for each dilution) in half-area 96-well plates in the presence of DEAE-dextran (12.5 μg/ml) for 48 hours at 37°C. Virus infectivity was measured by β-galactosidase activity (Promega, Madison, WI). Virus stocks were concentrated (20X) by ultracentrifugation over 20% (w/v) sucrose in 1X phosphate buffered saline (PBS) at 28,000 RPM for 2 hours in an SW-28 swinging bucket rotor (Sorvall, Thermofisher Scientific). Supernatants were decanted and pellets dried briefly before resuspension in PBS. Inactivation of virions was carried out using Aldrithiol-2 (AT-2) (34, 85). Briefly, 125 ul of sucrose-purified virus was incubated with 0.5 mM AT-2 in DMSO for 2hrs at 37ºC, followed by centrifugation at 13,000 rpm for 2 hours. The supernatant was discarded, and the pellet re-suspended in 125 ul PBS. Inactivation was confirmed by measuring infectivity in TZM.bl cells and Env content was checked by Western blotting.

Western blotting: To quantify and monitor the expression of Env in each virus preparation Western blot analyses were performed. The sucrose-purified virus particles were lysed, resolved by SDS-PAGE on 4–20% tris-glycine gels (Bio-Rad, Hercules, CA), and blotted onto membranes, which were then probed with antibodies. A cocktail of anti-human anti-gp120 MAbs (anti-V3: 391, 694, 2219, 2558; anti-C2: 841, 1006; anti-C5: 450, 670, 722; 1μg/ml each) was used to detect Env. MAb 91-5D (1μg/ml) was used to detect Gag p24. Membranes were developed with Clarity Western ECL Substrate (Bio-Rad, Hercules, CA) and imaged by a ChemiDoc Imaging System (Bio-Rad, Hercules, CA). Purified recombinant gp120 and p24 proteins were also loaded at a known concentration as controls

and quantification standards. Band intensities were quantified using the Image Lab Software Version 5.0 (Bio-Rad, Hercules, CA).

Coupling of fluorescent beads to virions: Sucrose-purified, inactivated virions were covalently coupled to carboxylate-modified microspheres (1.0 µm) using a two-step carbodiimide reaction with the xMAP Ab Coupling (AbC) Kit according to manufacturers' instructions (Luminex, Austin, TX). Carboxylated beads were coupled to 125 µl of 20X concentrated virus preparations (~36.4×10^9 beads per reaction). Briefly, the stock microspheres were vortexed and sonicated to resuspend and disperse the microspheres and 12 µl was transferred to tube containing 1200 ul of 1% BSA/1X PBS (per virus). The microspheres were washed twice with 500 µl of activation buffer followed by vortexing and sonication after each step. The microspheres were activated with 250 µL of activation buffer, 50 µL of 50 mg/ml Sulfo-NHS (N-hydroxysulfosuccinimide), 50 µL of 40 mg/mL ethyl dimethylaminopropyl carbodiimide hydrochloride (EDC) and incubated for 20 min at room temperature with end-to-end rotation. The microspheres were washed three times in activation buffer, then incubated with AT-2 inactivated virus in activation buffer for 2 h at room temperature. We typically used 125 µl volume of 20X concentrated virus that equals to 100-175 ng total. The microspheres were subsequently washed and resuspended in 1.2 mL of 0.1% BSA/PBS and stored at 4°C until ready to use.

Virus-associated Env binding assay (VAEBA): The coupled microspheres were dispensed into 96-well plate (10 µl/well) and blocked with 100 ul of 3% BSA for 30 mins at 4°C. Plates were centrifuged at 2000 x g for 10 minutes and the supernatant was discarded. The microspheres were incubated with serially diluted mAbs for 30 min at 37°C followed by addition of anti-human-biotin (1:500 in 0.1% BSA/PBS) and incubated in the

dark for 30 mins. Plates were washed 3 times with PBS and incubated with Streptavidin-PE (1:1000 in 0.1% BSA/PBS) for 30 min followed by resuspension in 200µl of 0.5% paraformaldehyde. Plates were washed 3 times with PBS after each step. Analysis was done with Attune NxT flow cytometer, and ≥30,000 events were collected in the phycoerythrin (PE)+ gate. Data analysis was carried out using FCS-Express software as follows: FITC positive microspheres were selected from a plot of forward-area vs. FITC (FSC-A/FITC-A) from which doublets were excluded in a forward scatter height vs forward scatter area plot (FSC-H/FSC-A). Geometric mean fluorescent intensity (MFI) of PE+ beads representing anti-Env-stained virus particles coupled to FITC microspheres, were quantified, and multiplied with percentage of PE-positive beads. This number was divided by 100 and reported as binding score (BS). Background BS, as determined from microspheres stained without primary antibodies was subtracted from all Env-mAb pairs. Area under the titration curves were also calculated for select data sets. MAbs were used at concentrations detailed in each figure legend.

For time-dependent binding study, the assay was performed as above using biotinylated mAbs that were incubated with the virus-coupled beads for different time (0, 15, 30, 45, 60 and 75 min) followed by Streptavidin-PE. Data was acquired by Attune flow cytometer as above.

For conformational epitope exposure in response to mAbs, virus coupled microspheres were pre-incubated with titrated mAbs for 30 min at 37°C. Plates were centrifuged and further incubated with biotinylated mAbs (PG9, VRC01 or 2219) for 30 min at 37°C followed by Streptavidin-PE. Data was acquired by Attune NxT flow cytometer as above.

Cell-associated Env binding assay. An assay to detect antibody binding to cell surface expressed Env was performed as described (66, 86). Briefly, monolayers of 293T cells (4 × 10^6) seeded in 100-mm tissue culture dishes were transfected with 20 μg of gp160 expression plasmid using jetPEI (DNA:jetPEI ratio of 1:3) following manufacturer's instructions (Polyplus, New York, NY). Transfected cells were incubated for 24 hours at 37°C, washed with PBS, detached with trypsin-free cell-dissociation buffer, and resuspended in PBS containing 2% BSA. Cells were stained with Live/dead fixable Aqua stain and distributed into 96-well round-bottom tissue culture plates (5x10^4/well) for individual staining reactions. Cells were incubated with mAbs at concentrations detailed in figure legends. For detection of mAb binding, biotinylated goat anti-Human IgG Fc (1:500) followed by streptavidin phycoerythrin (PE) (1:1000) was used. The cells were washed 3X with PBS-B (PBS plus 1%BSA) after each step and all incubation steps were performed on ice for 30 min. Cells were analyzed with a BD Fortessa flow cytometer, and 30,000 events were collected in the PE+ gate. Analysis was carried out using FCS-Express software as follows: 293T cells were selected from a plot of forward-area vs. side scatter-area (FSC-A/SSC-A) from which doublets were excluded in a forward scatter height vs forward scatter area plot (FSC-H/FSC-A). Live cells were selected by Aqua-negative gating, and geometric mean fluorescent intensity (MFI) of PE+ cells, representing anti-Env-stained cells, were quantified. Background MFI, as determined from cells stained without primary antibodies was subtracted from all Env-mAb pairs.

Neutralization assay. Virus neutralization was measured using a β-galactosidase-based assay (Promega) with TZM.bl target cells (62). Serial dilutions of mAbs were added to the virus in half-area 96-well plates (Costar, Corning, NY) and incubated for designated time

periods (0 min and 60 min) at 37°C. TZM.bl cells were then added along with DEAE-dextran (12.5 μg/ml; Sigma). After a 48-hour incubation for each assay condition, at 37°C and in a 5% CO2 incubator, the β-galactosidase activity was measured. Each condition was tested in duplicate. Assay controls included replicate wells of TZM.bl cells alone (cell control) and TZM.bl cells with virus alone (virus control). The highest antibody concentrations tested were based on known neutralization titers and varied per mAb. PG9 and 2219 were analyzed in the range of 50 μg/ml to 0.78 μg/ml, PGT145 was analyzed in the range of 5 μg/ml to 0.001 μg/ml, and NIH45-46 was analyzed in the range of 2.5 μg/ml to 0.004 μg/ml, while 830A and 3685 were tested in the range of 100 μg/ml to 0.006 μg/ml. Percent neutralization was determined on the basis of virus control under the specific assay condition. The virus input corresponded to titrated stocks yielding 150,000 to 200,000 relative luminescence units (RLU).

Statistical analysis: All statistical analyses were performed with GraphPad Prism 9.4.1 (GraphPad, San Diego, CA USA). ANOVA and Mann-Whitney t-tests were performed as appropriate and are mentioned in the figure legends.

Results

Detection of REJO Env on HIV-1 particles: Several methods have been developed that allow visualization of binding of HIV-1 particle to Abs in an effort to dissect the antigenic landscape of Env displayed on the virus particles. These assays rely on using fluorescent virus particles or using a two-pronged approach to capture and detect HIV-1 using different Abs (87-89). In this study we developed an assay that can be easily adapted to test any HIV-1 or other viruses without the need to produce fluorescent virus particles. The assay developed is based on (a) coupling the virions to fluorescent microspheres; (b) staining virions immobilized on microspheres with antibodies targeting different epitopes; (c) staining the resulting complex with anti-human biotin and streptavidin-PE; and (d) detecting Env-Ab interaction via flow cytometry (Figure 1A).

Initially, we used REJO, a T/F, clade B, tier 2, HIV-1 isolate and select monoclonal antibodies (mAbs) that recognize the conformational CD4bs (NIH45-46) and linear V3 (2219) epitopes on Env. A non-HIV-1 mAb 3685 was used as negative control. To optimize the amount of sucrose-pelleted virus required to couple with the microspheres we tested four different amounts (25, 50, 100 and 125 µl corresponding to ~35, 70, 142 and 177 ng total Env, respectively) of 20X concentrated virus preparations. The Env content was measured by Western blot (Supplementary Figure 1) as in (83, 84).

At 125 µl of virus, the positive control NIH45-46 binding was significantly enhanced while the negative control 3685 background binding levels were low (Figure 1B). Thus, based on the fold AUC change over the non-HIV-1 mAb 3685 we selected to use 125 µl of 20X concentrated virus preparation, equivalent to 177 ng Env. At this amount, the negative control mAb stained the virions minimally (1.7%) (Figure 1C). The mAb NIH45-

46 bound 84% REJO virions, while only 1.8% particles bound to V3 mAb 2219 (Figure 1C). Next, we used the assay to analyze the antigenic makeup of Env on the virus particles using the extended mAb panel (Table 1) that covers most of the major Env domains.

The virus bound microspheres were treated with titrated amounts of mAbs and the assay was conducted as outlined in the Methods section. All three V2i mAbs (697, 830A, and 2158) bound to the Env on virions, with mAb 830A exhibiting the strongest binding (Figures 2A-C). In contrast, trimer-preferring V2q bNAbs (PG9, PG16, and PGT145) and peptide recognizing V2p mAbs (CH58 and CH59) were unable to bind to the Env on virions (Figures 2A-C). The V3 specific mAbs 2219 and 2557 also did not show any binding (Figure 2). This aligns well with previous studies showing that the V3 loop that is located beneath V1V2 at the apical center of the Env trimer is occluded in closed Env conformations (90, 91). Recognition of CD4bs epitopes by most mAbs, except NIH45-46, was also negligible while PGT151 (gp120-gp41 interface) and gp41 MPER mAb 4E10 displayed efficient binding. Higher binding of MPER specific 4E10 mAb may be either due to lipid cross-reactivity, increased exposure of the gp41 base or presence of gp41 stumps (34, 92, 93). Notably, PGT151 binds only to properly formed, cleaved trimers, and its binding was comparable to V2i mAb 830A (94).

To compare the relative levels of each epitope exposed on the virus particles we calculated the AUC values from the titration curves. Figure 2B represents the overall presentation of different epitopes on the virions as measured by mAb binding. A similar pattern was also observed when binding scores of mAbs tested at the highest dilution were plotted (Figure 2C). Thus, for subsequent experiments we tested the binding of mAbs to virions at one dilution and present the results as binding scores (BS).

Exposure of Env epitopes on virions is similar regardless of the clade, tier, or infection stage: We next tested two other HIV-1 isolates: CMU06 (acute; clade AE, tier 2) and SF162 (chronic; clade B, tier 1) using the same panel of mAbs. Binding of mAbs to CMU06 was similar to REJO with most bNAb epitopes being masked (Figure 3A). Overall the binding strength of mAbs to SF162 Env on virions was lower compared to CMU06 and REJO. This may be due to the differences in the amount of Env as measured by Western blotting (Fig S1). The mAbs 830A, PGT151 and 4E10 bound strongly to their respective epitopes on both CMU06 an SF162 virions. Thus, these three epitopes were consistently accessible on all three viruses tested in this study. The binding of V2i mAb 2158 was greater in SF162 (tier 1) compared to CMU06 (tier 2). The V2i mAbs tested in this study were isolated from a HIV-1 clade B-infected patients and reacts better to clade B isolates compared to other HIV-1 from other clades. However, relatively lower binding of 2158 was also observed with REJO virus suggesting isolate specific differences in the exposure of epitopes. The CD4bs mAb NIH45-46 binding was low in the case of CMU06 and SF162 virions versus REJO. In contrast another CD4bs mAb 3BNC117 showed better binding to SF162 than the other two viruses. Negligible binding was seen with the negative control mAb 3685. Similar to REJO, little to no binding was seen with the mAbs targeting the V2q and V3 epitopes (Fig 3, 5).

Binding profile of mAbs to Env expressed on the cell surface is different than Env on virions: Binding of transiently expressed Env on cells to the various HIV-1 Env-directed antibodies is routinely used to assess and compare the epitopes displayed among different HIV-1 isolates. We transfected 293T cells with gp160 expressing plasmids and probed the

Env expressed on the cell surface with the mAbs in Table 1. A different profile was observed when staining of Env on virus particles was compared to Env expressed on transfected cells (Fig. 4). All mAbs tested bound to Env expressed on cells, while this was not the case with HIV-1 particles (Fig. 3 and 5). The V2q, V2p, and V3 mAbs which did not bind to the virions displayed efficient binding to cell surface expressed Env. Thus, Env recognized by V2q is efficiently expressed however the Env incorporation mechanism may impact its level and how it's displayed on the virion surface. In addition, the Env on producer cells may also be populated by uncleaved Env monomers at the cell surface that are not incorporated into virions (95), which may also account for differences in binding. The CD4bs mAbs also displayed greater binding to cell-surface Env compared with viral particles. Based on PGT151 binding, which binds only to properly formed, cleaved trimers (96), T/F isolate REJO has greater levels of trimeric Env compared to acute CMU06 and chronic SF162 isolates. Differences were also observed when the recognition of epitopes on virions vs cell surface were compared to other HIV-1 isolates (Fig. 4 and 5). Thus, the binding profile of mAbs to Env differs based on the location of the Env (cell surface vs virions). Most bNAb and V3 epitopes are masked on the virus-associated Env, while these epitopes are accessible on the Env expressed on transfected cells.

Prolonging the mAb-virion interaction time does not unmask the occluded epitopes: Binding of antibodies to Env is essential in order for them to neutralize the virus. In a typical standard neutralization assay, virus and mAbs are incubated for 1 hour at 37°C prior to adding the target cells. In our Env binding assay, mAbs were incubated for only 30 min at 37°C, prompting us to test if increasing the mAb-virus interaction time would facilitate

binding, especially for the mAbs (V2q, V3, and CD4bs) that did not appear to bind after 30 minutes.

Therefore, microspheres coupled with REJO virus were incubated with select V2i (830), V2q (PG9), V3 (2219), CD4bs (NIH45-46), or control mAb (3685) for various periods of time (0 to 75 min). The binding of mAbs to the Env on REJO virus was measured by flow cytometry (Fig. 6). Little binding to REJO Env was observed for all mAbs when no incubation (0 min) was allowed, but a significant linear increase in binding of 830A and NIH45-46 mAbs was detected over time (Fig. 6). The V2q mAb PG9 and V3 mAb 2219 showed no increase in binding to REJO Env at any time point, indicating that epitopes of these mAbs remained occluded on the virus even after 75 min incubation (Fig. 6). As expected no binding was detected by the negative control mAb 3685 at any time point.

Masked Env epitopes can be exposed by pre-binding of other mAbs. Next, we explored the possibility if microsphere-virion coupling method had any adverse effect that may explain the inability to detect any binding to these epitopes. If that stands correct then binding of PG9 or V3 2219 mAb will remain low on virions even under conditions that are known to conformationally unmask these epitopes (97, 98). We tested this idea by pre-treating the virus with select mAbs followed by detecting the binding of V3 (2219) and V2q (PG9) mAbs. We incubated the microsphere-coated virions first with mAbs (eg 697, 830A, 2158, 447, or 2219) to induce structural changes in Env. After washing away the unbound mAb, we probed for V2q epitope exposure using biotinylated PG9 mAb. Non-biotinylated PG9 and non-HIV-1 mAb 3685 were used as controls. As seen in Fig. 7, binding of all three V2i mAbs (697, 830A and 2158) presumably induced an allosteric

effect that exposed the PG9 binding epitopes. This concurs with the published study showing that V2i 830A and 2158 increases the binding of PG9 mAb on A244 gp120 (98). However, 697 did not induce similar increased binding in case of A244 gp120 (98). In contrast, the V3 mAbs, epitopes of which remain occluded on the functional Env on virions, did not alter PG9 binding and were comparable to the negative control mAb 3685. Since PG9 epitopes are also inaccessible on virions, no binding was seen in this control as well. Thus, PG9 epitopes are available but are masked on the virions. We next evaluated if V3 epitopes can be similarly exposed. The V3 loops are tucked beneath V1V2, thus Abs that induce any movement in the V1V2 loops such that they are displaced from their position should expose the V3 epitopes. We made the use of CD4bs mAbs: NIH45-46 that binds strongly to Env on virions, the non-neutralizing mAb 694 that is known to expose V3 loops, and the V2i mAb 830A (97, 98). Non-biotinylated 2219 and 3685 were used as controls. Binding of 830A and 694 exposed the V3 epitopes allowing the binding of biotinylated 2219 mAb. In contrast, NIH45-46, despite binding well to REJO virions failed to expose the 2219 epitope. The 2219 epitopes are not available on virions in the absence of allosteric alterations; thus no binding was detected. These data suggest that vulnerable epitopes such as those targeted by the bNAb PG9 are conformationally occluded on the Env displayed on the virion surface. Also, the coupling method had no observable negative impact on the accessibility of these epitopes.

Neutralization of REJO and CMU06 viruses by bNAbs: The findings above suggested that allosteric changes but not time can allow binding of the V2q mAb PG9. However, given the reported neutralization breadth and potency of PG9, the inability of PG9 to bind to the virus-associated Env was perplexing (67, 68), particularly since it is expected that

the Ab must bind to the target in order to exert its neutralization efficacy. This led us to speculate that perhaps the interaction of virus with the target cells induces similar changes in the Env that allows the bNAbs such as PG9 to bind to their epitopes. In such a case, the neutralization of HIV-1 with PG9 mAb should be similar in the presence or absence of a virus-mAb pre-incubation step.

Indeed, as seen in Fig. 8, bNAbs PG9 and PGT145 were able to neutralize REJO virus with equal efficacy independent of a pre-incubation step. Among the CD4bs mAbs, neutralization by 3BNC117 and NIH45-46 was also similar at both t =0 and 60 minutes while VRC01 had a slightly better neutralization at t =60 min (AUC 111) compared to t =0 (AUC 85); however, the difference was not statistically significant. These data suggest that interaction of virus with target cells appears to induce localized antigenic changes in virions allowing for bNAbs to latch on to their epitopes. This is the first time, to the best of our knowledge that the V2q and CD4bs mAbs tested here are shown to require pre-interaction of virus with target cells to exhibit their neutralization effect. Interestingly, mAbs such as 830A and 4E10 show strong binding to their respective epitopes on virions however these mAbs fail to neutralize the REJO virus. One possible explanation for this observation may be that the 830A and 4E10 epitopes that are available for binding on virions are associated with non-functional Env hence binding to these Env epitopes does not impact virus infection. Similar results were observed when neutralization of CMU06 virus was compared at t =0 vs 60 min. Regardless, these data highlight the importance of gaining a better understanding of the multiple mechanisms that are utilized by HIV-1 to avoid interaction with host mounted Abs and maintain infectivity.

4. Discussion

This study focused on investigating the antigenic landscape of HIV-1 Env on the infectious virus particles that are encountered by the host immune system. We used a flow cytometry-based bead assay to quantitate the relative levels of Env epitopes that are exposed on intact virions. Although bead-based assays have been reported before, our approach varies from previous assays in that it alleviates the requirement of producing fluorescent virus particles (89). In addition, other assays make use of two anti-HIV-1 Abs, one Ab to capture the virus particles and other Ab to detect binding (88). As shown in this study, application of two Abs may skew the results and fail to differentiate between the actual binding and binding due to the conformational changes in Env influenced by the capture Ab. Furthermore, the assay described in this study can be easily translated to study other viruses (e.g., SARS-CoV, Influenza etc.,) and antigens in different formats (eg gp120, gp140 etc).

Our findings show that epitopes targeted by mAbs like 830A (V2i), PGT151 (gp120-gp41 interface) and 4E10 (gp41) are present at relatively higher levels on the surface of REJO, CMU06 and SF162 viruses, suggesting that elements that regulate Env epitope abundance are likely to be conserved among isolates. In contrast, the V2q and V3 epitopes are inaccessible on the virus and remain so even when longer virion-mAb interaction times are allowed. The V2q and V3 epitopes become available for binding by mAbs only when conformational changes are inflicted. This is expected for V3 epitopes as V3 loops are suggested to be tucked underneath the V1V2 loops (99) and conformational changes such as movement or displacement of V1V2 can release V3 loop allowing for its recognition by V3 targeting mAbs (6). However, studies have also shown that the V3 loop can flicker in

and out of its tucked position without disrupting the V1V2 organization at the apex (99, 100). Even slight opening of the trimer apex can expose the highly immunogenic V3 loop (101). In such a case we would expect to observe some level of binding to V3 mAbs but, V3 mAbs (2219, 2557) tested here did not show any binding even when the REJO virus and mAb interaction time were extended up to 75 min. The V3 epitopes also remained occluded in SF162 which is highly sensitive to neutralization by these V3 mAbs (80). The SF162 Env is presumed to be in open conformation (102-104) however, based on the sensitivity of SF162 to neutralization by a family of mAbs that recognize an SF162 type-specific quaternary epitope that bridges the V2 and V3 domains (105-108), it has been suggested that this Env exists predominantly in the closed conformation (109); which may explain the masked V3 epitopes on SF162 in our assay. These data suggest that perhaps this tendency of V3 to flip in-and-out may vary among different HIV-1 isolates and was not applicable to the viruses tested here. Inability of V3 mAbs to bind to Env on virions was also surprising particularly for SF162 as SF162 is neutralized very potently by the V3 mAbs 2219 and 2557 with a reported IC50 < 0.39 µg/ml (80). These data suggest that the V2i Abs are not interacting with Env molecules that are required for viral entry and the V3 epitopes on functional Env are occluded from binding. Native-like Env trimers are the leading platform for HIV-1 vaccine design and several modifications have been made to reduce the Env metastability and exposure of the V3-loop (110-112). Understanding how the viruses retain the V3 in a tucked-in position may help these efforts.

The V2q mAbs showed no binding to V1V2 at the trimer apex on virions. Neutralization of HIV-1, or any other viral pathogen, minimally requires an initial

encounter with an Ab. The PG9, PG16, and PGT145 mAbs can efficiently neutralize REJO virus (83), thus lack of detectable binding was unexpected, particularly since V3 is shielded only when the native Env trimer is in the closed pre-fusion conformation: a conformation that is required for the binding of V2q mAbs (99, 113).

Our previously published study has shown that different mechanisms are involved in occluding the V1V2 and V3 epitopes (50). While V3 epitopes can become accessible after engagement of CD4 receptor as shown with soluble CD4, no substantial impact was observed on V2i epitopes. Again, V2i epitopes such as those targeted by the 830A mAb are abundantly available on the virions however both REJO and CMU06 viruses are resistant to neutralization by 830A mAb when tested under standard 1 hour incubation assay (50, 66, 83) and both viruses become neutralization sensitive if the virus-mAb incubation is allowed to continue to 24 hours prior to adding the target TZM.bl cells (66, 83). Thus, prolonged incubation time allows for conformational unmasking or allows Env breathing that may transiently expose the occluded epitopes. We attempted to apply this idea to expose the V2q mAb epitopes on virus particles. However, allosteric changes induced by binding of V2i mAbs, but not prolonged interaction time with virus, allowed PG9 mAb to bind to V2q epitopes on REJO virus. As both V2i and V2q mAbs bind V1V2 when V2C is in β-strand conformation (49, 114), the mechanism by which the binding of V2i helped expose V2q remains unknown. Likewise, we observed no significant differences in neutralization of REJO virus by the V2q mAbs and CD4bs, when the neutralization assay omitted the commonly adopted one-hour pre-incubation step (62, 115-121). These data suggest that HIV-1 interaction with target cells causes changes that allow for these bNAbs to bind to their target epitopes and neutralize virions. The TZM.bl cell

line that is widely used for neutralization assay in HIV-1 field is modified to express human CD4 and CCR5 receptors which allows the cells to be infected by HIV-1 (62). It is possible that CD4 engagement may be influencing epitope exposure and contributing to the observed effect, however we cannot rule out the possibility that there may be other contributors. It is also plausible that CD4 binding may promote or stabilize quaternary conformational changes in Env that may facilitate access of bNAbs to the Env. The increased binding of PG9 is not due to gp120 shedding as 830A and NIH45-46 epitopes are available for binding to the 830 and NIH45-46 mAbs respectively even after 75 min incubation. Thus, the exact mechanism is not known and remains to be explored. Also, we do not understand why the NIH45-46 epitopes are exposed better on REJO but not on CMU06 and SF162 and if it affords any advantage to REJO, which is a T/F isolate. Nonetheless, these data have implications for antibody neutralization strategies and highlight a previously unknown aspect of how the occluded bNAb epitopes on the virions may be unmasked allowing the mAbs to bind to their epitopes and block infection. Testing a broader mAb and virus panel will establish if all bNAbs and viruses use similar mechanism as those displayed here.

HIV-1 displays a low number of Env spikes (~10-14) per virion (122, 123), comprising both functional and non-functional Envs (36, 124). While the number of trimers required for productive infection remains inconclusive (88, 125), it is plausible that 1-2 functional spikes may be sufficient to initiate the infection process (21, 126, 127). In such a case, HIV-1 may have a mechanism that allows the distribution of non-functional Env in such a way that they surround the functional Env, thus protecting this Env form. Only displacing or inducing changes in these surrounding probably non-functional forms allows exposure

of the functional Env. This seems applicable in light of the recent cryo-EM data showing that trimers on virions appear to be randomly distributed with no apparent clustering or predisposition (128). Thus, camouflaging by non-functional Env forms may be a way for HIV-1 to shield its functional Env, which is exposed only after conformational unmasking.

In summary, we show that only select Env epitopes are exposed on the HIV-1 surface, with V2i epitopes being the most abundant which may provide an explanation as to why Abs against these immunogenic epitopes are more readily elicited during infection (74, 75, 78, 79, 129-133). However, V3 Abs are also efficiently elicited during infection and via vaccination. Thus, the reason why the V3 epitopes on virions were not recognized by the mAbs tested herein remains unanswered. An indication that different HIV isolates can exhibit similar patterns of mAb binding regardless of the clade or tier suggest that similar mechanisms are at play to maintain the balance between the amount of functional and non-functional Env that gets incorporated into virus particles. We also show that interaction with cells is required for the bNAbs to be able to access their epitopes on virus particles. It will be interesting to know if other viruses for e.g., SARS-COV2, Influenza etc have similar requirements of interacting with host cells in order for the virus-specific neutralizing Abs to exert their effect, thus alleviating the one hour pre-incubation step or if this is specific for HIV-1 alone. These results may have important implications for HIV-1 vaccine design and for understanding the humoral response to HIV infection.

Acknowledgments:

The authors would like to thank Dr. Susan Zolla-Pazner, and Ms. Xiaomei Liu for providing HIV-1-specific mAbs.

Figure Legends

Figure. 1. Virus-binding assay for detection of antibody binding to Env expressed on virions. (A) Schematic of the assay; (B) Optimization of virus amount to be coupled to the microspheres; (C) Representative dot plots and histogram showing the gating strategy for analysis of antibodies binding to virus particle by flow cytometry. The mAbs were tested at following concentrations: NIH45-46 at 5 μg/ml; 2219 and 3685 at 50 μg/ml. 1°, primary; 2° secondary.

Figure 2. Binding of mAbs to Env on REJO virions. (A) Microspheres coupled to REJO virus were incubated with serially diluted mAbs targeting different Env epitopes. (B) Area under the curve (AUC) was calculated from the mAb titration curves in panel A and plotted. (C) Binding scores (BS) were calculated by multiplying the percent gated PE positive beads with the geometric mean fluorescence intensity (MFI) of each mAb tested at a single dilution. This value was divided by one hundred and is plotted. Virus-coupled microspheres stained with biotin and PE alone were used to set the background BS and are subtracted from all values.

Figure 3. Binding of mAbs to Env on virions. Microspheres coupled to (A) CMU06 and (B) SF162 viruses were incubated with mAbs targeting different Env epitopes. Binding scores (BS) were calculated by multiplying the percent gated PE positive beads with the geometric mean fluorescence intensity (MFI) of each mAb tested at the single dilution. This value was divided by one hundred and is plotted. Virus coupled microspheres stained with biotin and PE alone were used to set the background BS and subtracted. The mAbs were tested at following concentrations: 697, 830A, 2158, 3685 at 100 μg/ml; 2219, 2557

at 50 μg/ml; PG9, PG16, PGT145, CH59, VRC01, 3BNC117 at 25 μg/ml; 4E10 at 20 μg/ml; PGT151 at 10 μg/ml; NIH45-46 at 5 μg/ml. X, not tested.

Figure 4. Binding of mAbs to trimeric Env expressed on cell surface. (A) 293T cells were transiently transfected with plasmid encoding for full length gp160. Cells were analyzed for binding of different mAbs 24-hours post-transfection. Binding scores (BS) were calculated by multiplying the percent gated PE positive cells with geometric mean fluorescence intensity (MFI) of each mAb tested at the single dilution. This value was divided by one hundred and is plotted. Transfected cells stained with biotin and PE alone were used to set the background BS and subtracted. X, not tested. The mAbs were tested at following concentrations: 697, 830A, 2158, 3685 at 100 μg/ml; 2219, 2557 at 50 μg/ml; PG9, PG16, PGT145, PGDM1400, CH59, VRC01, 3BNC117, b12 at 25 μg/ml; 4E10, 2F5 at 20 μg/ml; PGT151 at 10 μg/ml; NIH45-46 at 5 μg/ml. X, not tested.

Figure 5. Comparison of binding of mAbs to Env on virions and cell surface. Binding data in figures 2, 3 and 4 was normalized and shown as fold change over negative control mAb 3685. X, not tested.

Figure 6. Time-dependent increase of Env binding. Microspheres coupled to REJO virus particles were treated with mAbs at 37°C for various time from 0 to 75 min. Binding was detected as in Figure 2 and binding scores (BS) are shown. The mAbs were tested at following concentrations: 830A, 3685 at 100 μg/ml; 2219 at 50 μg/ml; PG9 at 25 μg/ml; NIH45-46 at 2.5 μg/ml. ****, $p = <0.0001$; **, $p = 0.0026$ vs $t = 0$ min by ANOVA.

Figure 7. Changes in reactivity of PG9 and 2219 mAbs. Microspheres coupled with REJO virus were incubated with titrated amounts of antibodies followed by biotinylated

V2q mAb PG9 (25 μg/ml) or biotinylated V3 mAb 2219 (50 μg/ml). Binding was detected with streptavidin-PE. **** $p < 0.0001$ by ANOVA.

Figure 8. Neutralization of REJO virus. Virus neutralization was measured after REJO was incubated with serially diluted mAbs for the designated period of time at 37°C prior to the addition of TZM-bl target cells. Virus infectivity was assessed 48 h later based on β-galactosidase activity. (A) Neutralization curves are shown. Means and standard errors calculated from two different experiments (each in duplicate) are shown. Statistical analyses were performed on the neutralization curves reaching ≥50%. Comparison is made between neutralization curves at T = 0 vs T = 60 minutes. P= ns, not significant by nonparametric Mann-Whitney t-test. (B) Area under the neutralization curves were calculated and plotted as bar graph. Statistical analysis was performed on AUC graph by ANOVA (P = 0.99; ns, not significant).

Figure 9. Neutralization of CMU06 virus. Virus neutralization was measured after CMU06 was incubated with serially diluted mAbs for the designated period of time at 37°C prior to the addition of TZM-bl target cells. Virus infectivity was assessed 48 h later based on β-galactosidase activity. (A) Neutralization curves are shown. Means and standard errors calculated from two different experiments (each in duplicate) are shown. Statistical analyses were performed on the neutralization curves reaching ≥50%. Comparison is made between neutralization curves at T = 0 vs T = 60 minutes. P= ns, not significant by nonparametric Mann-Whitney t-test. (B) Area under the neutralization curves were calculated and plotted as bar graph. Statistical analysis was performed on AUC graph by ANOVA (P = 0.99; ns, not significant)

Supplementary Figure 1. Measurement of Env in virus preparations by Western blot. (A) Viruses produced in 293T cells, were concentrated (20X) by sucrose pelleting. 4 µl of each 20X concentrated virus particles were lysed and analyzed by SDS-PAGE (4–20%) and Western blot. An anti-gp120 MAb cocktail (V3: 391/95-D, 694/98-D, 2219, 2558; C2: 847-D, 1006-30D; C5: 450-D, 670-D) was used to quantitate the levels of Env associated with virions. REJO gp120 protein loaded at different concentrations was used as standard. The band density of REJO gp120 protein was used to generate the linear curve (B) and to calculate the amount of Env in each virus preparation.

Funding: "This research was funded by NIH R01 grant (AI140909 to C.U.).

Institutional Review Board Statement: "Not applicable".

Informed Consent Statement: "Not applicable".

Data Availability Statement: All available data are presented in the article.

Conflicts of Interest: "The authors declare no conflict of interest."

References

1. Wyatt R, Sodroski J. 1998. The HIV-1 envelope glycoproteins: fusogens, antigens, and immunogens. Science 280:1884-8.
2. Munro JB, Gorman J, Ma X, Zhou Z, Arthos J, Burton DR, Koff WC, Courter JR, Smith AB, 3rd, Kwong PD, Blanchard SC, Mothes W. 2014. Conformational dynamics of single HIV-1 envelope trimers on the surface of native virions. Science 346:759-63.
3. Ma X, Lu M, Gorman J, Terry DS, Hong X, Zhou Z, Zhao H, Altman RB, Arthos J, Blanchard SC, Kwong PD, Munro JB, Mothes W. 2018. HIV-1 Env trimer opens through an asymmetric intermediate in which individual protomers adopt distinct conformations. Elife 7.
4. Guzzo C, Zhang P, Liu Q, Kwon AL, Uddin F, Wells AI, Schmeisser H, Cimbro R, Huang J, Doria-Rose N, Schmidt SD, Dolan MA, Connors M, Mascola JR, Lusso P. 2018. Structural Constraints at the Trimer Apex Stabilize the HIV-1 Envelope in a Closed, Antibody-Protected Conformation. mBio 9.
5. Wang Q, Finzi A, Sodroski J. 2020. The Conformational States of the HIV-1 Envelope Glycoproteins. Trends Microbiol 28:655-667.
6. Wang H, Barnes CO, Yang Z, Nussenzweig MC, Bjorkman PJ. 2018. Partially Open HIV-1 Envelope Structures Exhibit Conformational Changes Relevant for Coreceptor Binding and Fusion. Cell Host Microbe 24:579-592 e4.
7. Tran EE, Borgnia MJ, Kuybeda O, Schauder DM, Bartesaghi A, Frank GA, Sapiro G, Milne JL, Subramaniam S. 2012. Structural mechanism of trimeric HIV-1 envelope glycoprotein activation. PLoS Pathog 8:e1002797.
8. Ward AB, Wilson IA. 2017. The HIV-1 envelope glycoprotein structure: nailing down a moving target. Immunol Rev 275:21-32.
9. Stadtmueller BM, Bridges MD, Dam KM, Lerch MT, Huey-Tubman KE, Hubbell WL, Bjorkman PJ. 2018. DEER Spectroscopy Measurements Reveal Multiple Conformations of HIV-1 SOSIP Envelopes that Show Similarities with Envelopes on Native Virions. Immunity 49:235-246 e4.
10. Liang Y, Guttman M, Davenport TM, Hu SL, Lee KK. 2016. Probing the Impact of Local Structural Dynamics of Conformational Epitopes on Antibody Recognition. Biochemistry 55:2197-213.
11. Davenport TM, Guttman M, Guo W, Cleveland B, Kahn M, Hu SL, Lee KK. 2013. Isolate-specific differences in the conformational dynamics and antigenicity of HIV-1 gp120. J Virol 87:10855-73.
12. Ivan B, Sun Z, Subbaraman H, Friedrich N, Trkola A. 2019. CD4 occupancy triggers sequential pre-fusion conformational states of the HIV-1 envelope trimer with relevance for broadly neutralizing antibody activity. PLoS Biol 17:e3000114.
13. Kwong PD, Doyle ML, Casper DJ, Cicala C, Leavitt SA, Majeed S, Steenbeke TD, Venturi M, Chaiken I, Fung M, Katinger H, Parren PW, Robinson J, Van Ryk D, Wang L, Burton DR, Freire E, Wyatt R, Sodroski J, Hendrickson WA, Arthos J. 2002. HIV-1 evades antibody-mediated neutralization through conformational masking of receptor-binding sites. Nature 420:678-82.
14. Doria-Rose NA, Schramm CA, Gorman J, Moore PL, Bhiman JN, DeKosky BJ, Ernandes MJ, Georgiev IS, Kim HJ, Pancera M, Staupe RP, Altae-Tran HR, Bailer

RT, Crooks ET, Cupo A, Druz A, Garrett NJ, Hoi KH, Kong R, Louder MK, Longo NS, McKee K, Nonyane M, O'Dell S, Roark RS, Rudicell RS, Schmidt SD, Sheward DJ, Soto C, Wibmer CK, Yang Y, Zhang Z, Program NCS, Mullikin JC, Binley JM, Sanders RW, Wilson IA, Moore JP, Ward AB, Georgiou G, Williamson C, Abdool Karim SS, Morris L, Kwong PD, Shapiro L, Mascola JR. 2014. Developmental pathway for potent V1V2-directed HIV-neutralizing antibodies. Nature 509:55-62.

15. McLellan JS, Pancera M, Carrico C, Gorman J, Julien JP, Khayat R, Louder R, Pejchal R, Sastry M, Dai K, O'Dell S, Patel N, Shahzad-ul-Hussan S, Yang Y, Zhang B, Zhou T, Zhu J, Boyington JC, Chuang GY, Diwanji D, Georgiev I, Kwon YD, Lee D, Louder MK, Moquin S, Schmidt SD, Yang ZY, Bonsignori M, Crump JA, Kapiga SH, Sam NE, Haynes BF, Burton DR, Koff WC, Walker LM, Phogat S, Wyatt R, Orwenyo J, Wang LX, Arthos J, Bewley CA, Mascola JR, Nabel GJ, Schief WR, Ward AB, Wilson IA, Kwong PD. 2011. Structure of HIV-1 gp120 V1/V2 domain with broadly neutralizing antibody PG9. Nature 480:336-43.

16. Walker LM, Phogat SK, Chan-Hui PY, Wagner D, Phung P, Goss JL, Wrin T, Simek MD, Fling S, Mitcham JL, Lehrman JK, Priddy FH, Olsen OA, Frey SM, Hammond PW, Kaminsky S, Zamb T, Moyle M, Koff WC, Poignard P, Burton DR. 2009. Broad and potent neutralizing antibodies from an African donor reveal a new HIV-1 vaccine target. Science 326:285-9.

17. Walker LM, Huber M, Doores KJ, Falkowska E, Pejchal R, Julien JP, Wang SK, Ramos A, Chan-Hui PY, Moyle M, Mitcham JL, Hammond PW, Olsen OA, Phung P, Fling S, Wong CH, Phogat S, Wrin T, Simek MD, Koff WC, Wilson IA, Burton DR, Poignard P. 2011. Broad neutralization coverage of HIV by multiple highly potent antibodies. Nature 477:466-70.

18. Sok D, van Gils MJ, Pauthner M, Julien J-P, Saye-Francisco KL, Hsueh J, Briney B, Lee JH, Le KM, Lee PS. 2014. Recombinant HIV envelope trimer selects for quaternary-dependent antibodies targeting the trimer apex. Proceedings of the National Academy of Sciences 111:17624-17629.

19. Gallo SA, Finnegan CM, Viard M, Raviv Y, Dimitrov A, Rawat SS, Puri A, Durell S, Blumenthal R. 2003. The HIV Env-mediated fusion reaction. Biochim Biophys Acta 1614:36-50.

20. Eckert DM, Kim PS. 2001. Mechanisms of viral membrane fusion and its inhibition. Annu Rev Biochem 70:777-810.

21. Brandenberg OF, Magnus C, Rusert P, Regoes RR, Trkola A. 2015. Different infectivity of HIV-1 strains is linked to number of envelope trimers required for entry. PLoS Pathog 11:e1004595.

22. Bosch V, Pawlita M. 1990. Mutational analysis of the human immunodeficiency virus type 1 env gene product proteolytic cleavage site. Journal of Virology 64:2337-2344.

23. Fennie C, Lasky LA. 1989. Model for intracellular folding of the human immunodeficiency virus type 1 gp120. Journal of Virology 63:639-646.

24. Li Y, Luo L, Thomas DY, Kang CY. 2000. The HIV-1 Env protein signal sequence retards its cleavage and down- regulates the glycoprotein folding. Virology 272:417-428.

25. Willey RL, Bonifacino JS, Potts BJ, Martin MA, Klausner RD. 1988. Biosynthesis, cleavage, and degradation of the human immunodeficiency virus 1 envelope glycoprotein gp160. Proc Natl Acad Sci U S A 85:9580-4.
26. Martoglio B, Dobberstein B. 1998. Signal sequences: more than just greasy peptides. Trends Cell Biol 8:410-5.
27. Land A, Zonneveld D, Braakman I. 2003. Folding of HIV-1 envelope glycoprotein involves extensive isomerization of disulfide bonds and conformation-dependent leader peptide cleavage. FASEB J 17:1058-67.
28. Li Y, Bergeron JJ, Luo L, Ou WJ, Thomas DY, Kang CY. 1996. Effects of inefficient cleavage of the signal sequence of HIV-1 gp 120 on its association with calnexin, folding, and intracellular transport. Proc Natl Acad Sci U S A 93:9606-11.
29. Li Y, Luo L, Rasool N, Kang CY. 1993. Glycosylation is necessary for the correct folding of human immunodeficiency virus gp120 in CD4 binding. J Virol 67:584-8.
30. Bosch V, Pawlita M. 1990. Mutational analysis of the human immunodeficiency virus type 1 env gene product proteolytic cleavage site. J Virol 64:2337-44.
31. Decroly E, Vandenbranden M, Ruysschaert JM, Cogniaux J, Jacob GS, Howard SC, Marshall G, Kompelli A, Basak A, Jean F, Lazure C, Benjannet S, Chrétien M, Day R, Seidah NG. 1994. The convertases furin and PC1 can both cleave the human immunodeficiency virus (HIV)-1 envelope glycoprotein gp160 into gp120 (HIV-I SU) and gp41 (HIV-I TM). Journal of Biological Chemistry 269:12240-12247.
32. Kantanen ML, Leinikki P, Kuismanen E. 1995. Endoproteolytic cleavage of HIV-1 gp160 envelope precursor occurs after exit from the trans-Golgi network (TGN). Archives of Virology 140:1441-1449.
33. Pfeiffer T, Zentgraf H, Freyaldenhoven B, Bosch V. 1997. Transfer of endoplasmic reticulum and Golgi retention signals to human immunodeficiency virus type 1 gp 160 inhibits intracellular transport and proteolytic processing of viral glycoprotein but does not influence the cellular site of virus particle budding. Journal of General Virology 78:1745-1753.
34. Stieh DJ, King DF, Klein K, Aldon Y, McKay PF, Shattock RJ. 2015. Discrete partitioning of HIV-1 Env forms revealed by viral capture. Retrovirology 12:81.
35. Crooks ET, Tong T, Osawa K, Binley JM. 2011. Enzyme digests eliminate nonfunctional Env from HIV-1 particle surfaces, leaving native Env trimers intact and viral infectivity unaffected. J Virol 85:5825-39.
36. Moore PL, Crooks ET, Porter L, Zhu P, Cayanan CS, Grise H, Corcoran P, Zwick MB, Franti M, Morris L, Roux KH, Burton DR, Binley JM. 2006. Nature of nonfunctional envelope proteins on the surface of human immunodeficiency virus type 1. J Virol 80:2515-28.
37. Cao L, Pauthner M, Andrabi R, Rantalainen K, Berndsen Z, Diedrich JK, Menis S, Sok D, Bastidas R, Park SR, Delahunty CM, He L, Guenaga J, Wyatt RT, Schief WR, Ward AB, Yates JR, 3rd, Burton DR, Paulson JC. 2018. Differential processing of HIV envelope glycans on the virus and soluble recombinant trimer. Nat Commun 9:3693.
38. Zolla-Pazner S, DeCamp A, Gilbert PB, Williams C, Yates NL, Williams WT, Howington R, Fong Y, Morris DE, Soderberg KA, Irene C, Reichman C, Pinter A,

Parks R, Pitisuttithum P, Kaewkungwal J, Rerks-Ngarm S, Nitayaphan S, Andrews C, O'Connell RJ, Yang ZY, Nabel GJ, Kim JH, Michael NL, Montefiori DC, Liao HX, Haynes BF, Tomaras GD. 2014. Vaccine-induced IgG antibodies to V1V2 regions of multiple HIV-1 subtypes correlate with decreased risk of HIV-1 infection. PLoS ONE 9.

39. Zolla-Pazner S, Cohen S, Pinter A, Krachmarov C, Wrin T, Wang S, Lu S. 2009. Cross-clade neutralizing antibodies against HIV-1 induced in rabbits by focusing the immune response on a neutralizing epitope. Virology 392:82-93.

40. Visciano ML, Tuen M, Gorny MK, Hioe CE. 2008. In vivo alteration of humoral responses to HIV-1 envelope glycoprotein gp120 by antibodies to the CD4-binding site of gp120. Virology 372:409-420.

41. Lynch RM, Rong R, Boliar S, Sethi A, Li B, Mulenga J, Allen S, Robinson JE, Gnanakaran S, Derdeyn CA. 2011. The B cell response is redundant and highly focused on V1V2 during early subtype C infection in a Zambian seroconverter. Journal of Virology 85:905-915.

42. Kumar R, Tuen M, Liu J, Nàdas A, Pan R, Kong X, Hioe CE. 2013. Elicitation of broadly reactive antibodies against glycan-modulated neutralizing V3 epitopes of HIV-1 by immune complex vaccines. Vaccine 31:5413-5421.

43. Hessell AJ, McBurney S, Pandey S, Sutton W, Liu L, Li L, Totrov M, Zolla-Pazner S, Haigwood NL, Gorny MK. 2016. Induction of neutralizing antibodies in rhesus macaques using V3 mimotope peptides. Vaccine 34:2713-2721.

44. Hessell AJ, Malherbe DC, Pissani F, McBurney S, Krebs SJ, Gomes M, Pandey S, Sutton WF, Burwitz BJ, Gray M, Robins H, Park BS, Sacha JB, La Branche CC, Fuller DH, Montefiori DC, Stamatatos L, Sather DN, Haigwood NL. 2016. Achieving potent autologous neutralizing antibody responses against tier 2 HIV-1 viruses by strategic selection of envelope immunogens. Journal of Immunology 196:3064-3078.

45. Davis KL, Gray ES, Moore PL, Decker JM, Salomon A, Montefiori DC, Graham BS, Keefer MC, Pinter A, Morris L, Hahn BH, Shaw GM. 2009. High titer HIV-1 V3-specific antibodies with broad reactivity but low neutralizing potency in acute infection and following vaccination. Virology 387:414-426.

46. Davis KL, Bibollet-Ruche F, Li H, Decker JM, Kutsch O, Morris L, Salomon A, Pinter A, Hoxie JA, Hahn BH, Kwong PD, Shaw GM. 2009. Human immunodeficiency virus type 2 (HIV-2)/HIV-1 envelope chimeras detect high titers of broadly reactive HIV-1 V3-specific antibodies in human plasma. Journal of Virology 83:1240-1259.

47. Carbonetti S, Oliver BG, Glenn J, Stamatatos L, Sather DN. 2014. Soluble HIV-1 envelope immunogens derived from an elite neutralizer elicit cross-reactive V1V2 antibodies and low potency neutralizing antibodies. PLoS ONE 9.

48. Parker Miller E, Finkelstein MT, Erdman MC, Seth PC, Fera D. 2021. A Structural Update of Neutralizing Epitopes on the HIV Envelope, a Moving Target. Viruses 13.

49. Pan R, Gorny MK, Zolla-Pazner S, Kong XP. 2015. The V1V2 Region of HIV-1 gp120 Forms a Five-Stranded Beta Barrel. J Virol 89:8003-10.

50. Upadhyay C, Mayr LM, Zhang J, Kumar R, Gorny MK, Nadas A, Zolla-Pazner S, Hioe CE. 2014. Distinct mechanisms regulate exposure of neutralizing epitopes in the V2 and V3 loops of HIV-1 envelope. J Virol 88:12853-65.
51. Aiyegbo MS, Shmelkov E, Dominguez L, Goger M, Battacharya S, deCamp AC, Gilbert PB, Berman PW, Cardozo T. 2017. Peptide Targeted by Human Antibodies Associated with HIV Vaccine-Associated Protection Assumes a Dynamic alpha-Helical Structure. PLoS One 12:e0170530.
52. Liao HX, Bonsignori M, Alam SM, McLellan JS, Tomaras GD, Moody MA, Kozink DM, Hwang KK, Chen X, Tsao CY, Liu P, Lu X, Parks RJ, Montefiori DC, Ferrari G, Pollara J, Rao M, Peachman KK, Santra S, Letvin NL, Karasavvas N, Yang ZY, Dai K, Pancera M, Gorman J, Wiehe K, Nicely NI, Rerks-Ngarm S, Nitayaphan S, Kaewkungwal J, Pitisuttithum P, Tartaglia J, Sinangil F, Kim JH, Michael NL, Kepler TB, Kwong PD, Mascola JR, Nabel GJ, Pinter A, Zolla-Pazner S, Haynes BF. 2013. Vaccine induction of antibodies against a structurally heterogeneous site of immune pressure within HIV-1 envelope protein variable regions 1 and 2. Immunity 38:176-86.
53. Wibmer CK, Richardson SI, Yolitz J, Cicala C, Arthos J, Moore PL, Morris L. 2018. Common helical V1V2 conformations of HIV-1 Envelope expose the alpha4beta7 binding site on intact virions. Nat Commun 9:4489.
54. Pancera M, Zhou T, Druz A, Georgiev IS, Soto C, Gorman J, Huang J, Acharya P, Chuang GY, Ofek G, Stewart-Jones GB, Stuckey J, Bailer RT, Joyce MG, Louder MK, Tumba N, Yang Y, Zhang B, Cohen MS, Haynes BF, Mascola JR, Morris L, Munro JB, Blanchard SC, Mothes W, Connors M, Kwong PD. 2014. Structure and immune recognition of trimeric pre-fusion HIV-1 Env. Nature 514:455-61.
55. Lee JH, Andrabi R, Su CY, Yasmeen A, Julien JP, Kong L, Wu NC, McBride R, Sok D, Pauthner M, Cottrell CA, Nieusma T, Blattner C, Paulson JC, Klasse PJ, Wilson IA, Burton DR, Ward AB. 2017. A Broadly Neutralizing Antibody Targets the Dynamic HIV Envelope Trimer Apex via a Long, Rigidified, and Anionic beta-Hairpin Structure. Immunity 46:690-702.
56. Sok D, van Gils MJ, Pauthner M, Julien JP, Saye-Francisco KL, Hsueh J, Briney B, Lee JH, Le KM, Lee PS, Hua Y, Seaman MS, Moore JP, Ward AB, Wilson IA, Sanders RW, Burton DR. 2014. Recombinant HIV envelope trimer selects for quaternary-dependent antibodies targeting the trimer apex. Proc Natl Acad Sci U S A 111:17624-9.
57. Li Y, O'Dell S, Walker LM, Wu X, Guenaga J, Feng Y, Schmidt SD, McKee K, Louder MK, Ledgerwood JE, Graham BS, Haynes BF, Burton DR, Wyatt RT, Mascola JR. 2011. Mechanism of neutralization by the broadly neutralizing HIV-1 monoclonal antibody VRC01. J Virol 85:8954-67.
58. Klein F, Gaebler C, Mouquet H, Sather DN, Lehmann C, Scheid JF, Kraft Z, Liu Y, Pietzsch J, Hurley A, Poignard P, Feizi T, Morris L, Walker BD, Fatkenheuer G, Seaman MS, Stamatatos L, Nussenzweig MC. 2012. Broad neutralization by a combination of antibodies recognizing the CD4 binding site and a new conformational epitope on the HIV-1 envelope protein. J Exp Med 209:1469-79.
59. Mayr LM, Decoville T, Schmidt S, Laumond G, Klingler J, Ducloy C, Bahram S, Zolla-Pazner S, Moog C. 2017. Non-neutralizing Antibodies Targeting the V1V2

Domain of HIV Exhibit Strong Antibody-Dependent Cell-mediated Cytotoxic Activity. Sci Rep 7:12655.

60. Mayr LM, Su B, Moog C. 2017. Non-Neutralizing Antibodies Directed against HIV and Their Functions. Front Immunol 8:1590.

61. Mascola JR, D'Souza P, Gilbert P, Hahn BH, Haigwood NL, Morris L, Petropoulos CJ, Polonis VR, Sarzotti M, Montefiori DC. 2005. Recommendations for the design and use of standard virus panels to assess neutralizing antibody responses elicited by candidate human immunodeficiency virus type 1 vaccines. J Virol 79:10103-7.

62. Montefiori DC. 2005. Evaluating neutralizing antibodies against HIV, SIV, and SHIV in luciferase reporter gene assays. Curr Protoc Immunol Chapter 12:Unit 12 11.

63. Montefiori DC, Karnasuta C, Huang Y, Ahmed H, Gilbert P, de Souza MS, McLinden R, Tovanabutra S, Laurence-Chenine A, Sanders-Buell E, Moody MA, Bonsignori M, Ochsenbauer C, Kappes J, Tang H, Greene K, Gao H, LaBranche CC, Andrews C, Polonis VR, Rerks-Ngarm S, Pitisuttithum P, Nitayaphan S, Kaewkungwal J, Self SG, Berman PW, Francis D, Sinangil F, Lee C, Tartaglia J, Robb ML, Haynes BF, Michael NL, Kim JH. 2012. Magnitude and breadth of the neutralizing antibody response in the RV144 and Vax003 HIV-1 vaccine efficacy trials. J Infect Dis 206:431-41.

64. Platt EJ, Wehrly K, Kuhmann SE, Chesebro B, Kabat D. 1998. Effects of CCR5 and CD4 cell surface concentrations on infections by macrophagetropic isolates of human immunodeficiency virus type 1. J Virol 72:2855-64.

65. Ochsenbauer C, Edmonds TG, Ding H, Keele BF, Decker J, Salazar MG, Salazar-Gonzalez JF, Shattock R, Haynes BF, Shaw GM, Hahn BH, Kappes JC. 2012. Generation of transmitted/founder HIV-1 infectious molecular clones and characterization of their replication capacity in CD4 T lymphocytes and monocyte-derived macrophages. J Virol 86:2715-28.

66. Upadhyay C, Feyznezhad R, Cao L, Chan KW, Liu K, Yang W, Zhang H, Yolitz J, Arthos J, Nadas A, Kong XP, Zolla-Pazner S, Hioe CE. 2020. Signal peptide of HIV-1 envelope modulates glycosylation impacting exposure of V1V2 and other epitopes. PLoS Pathog 16:e1009185.

67. Walker LM, Phogat SK, Chan-Hui PY, Wagner D, Phung P, Goss JL, Wrin T, Simek MD, Fling S, Mitcham JL, Lehrman JK, Priddy FH, Olsen OA, Frey SM, Hammond PW, Protocol GPI, Kaminsky S, Zamb T, Moyle M, Koff WC, Poignard P, Burton DR. 2009. Broad and potent neutralizing antibodies from an African donor reveal a new HIV-1 vaccine target. Science 326:285-9.

68. Wu X, Yang ZY, Li Y, Hogerkorp CM, Schief WR, Seaman MS, Zhou T, Schmidt SD, Wu L, Xu L, Longo NS, McKee K, O'Dell S, Louder MK, Wycuff DL, Feng Y, Nason M, Doria-Rose N, Connors M, Kwong PD, Roederer M, Wyatt RT, Nabel GJ, Mascola JR. 2010. Rational design of envelope identifies broadly neutralizing human monoclonal antibodies to HIV-1. Science 329:856-61.

69. Barbas CF, 3rd, Bjorling E, Chiodi F, Dunlop N, Cababa D, Jones TM, Zebedee SL, Persson MA, Nara PL, Norrby E, et al. 1992. Recombinant human Fab fragments neutralize human type 1 immunodeficiency virus in vitro. Proc Natl Acad Sci U S A 89:9339-43.

70. Scheid JF, Mouquet H, Ueberheide B, Diskin R, Klein F, Oliveira TY, Pietzsch J, Fenyo D, Abadir A, Velinzon K, Hurley A, Myung S, Boulad F, Poignard P, Burton DR, Pereyra F, Ho DD, Walker BD, Seaman MS, Bjorkman PJ, Chait BT, Nussenzweig MC. 2011. Sequence and structural convergence of broad and potent HIV antibodies that mimic CD4 binding. Science 333:1633-7.
71. Thali M, Moore JP, Furman C, Charles M, Ho DD, Robinson J, Sodroski J. 1993. Characterization of conserved human immunodeficiency virus type 1 gp120 neutralization epitopes exposed upon gp120-CD4 binding. J Virol 67:3978-88.
72. Buchacher A, Predl R, Strutzenberger K, Steinfellner W, Trkola A, Purtscher M, Gruber G, Tauer C, Steindl F, Jungbauer A, et al. 1994. Generation of human monoclonal antibodies against HIV-1 proteins; electrofusion and Epstein-Barr virus transformation for peripheral blood lymphocyte immortalization. AIDS Res Hum Retroviruses 10:359-69.
73. Stiegler G, Kunert R, Purtscher M, Wolbank S, Voglauer R, Steindl F, Katinger H. 2001. A potent cross-clade neutralizing human monoclonal antibody against a novel epitope on gp41 of human immunodeficiency virus type 1. AIDS Res Hum Retroviruses 17:1757-65.
74. Gorny MK, Moore JP, Conley AJ, Karwowska S, Sodroski J, Williams C, Burda S, Boots LJ, Zolla-Pazner S. 1994. Human anti-V2 monoclonal antibody that neutralizes primary but not laboratory isolates of human immunodeficiency virus type 1. J Virol 68:8312-20.
75. Gorny MK, Pan R, Williams C, Wang XH, Volsky B, O'Neal T, Spurrier B, Sampson JM, Li L, Seaman MS, Kong XP, Zolla-Pazner S. 2012. Functional and immunochemical cross-reactivity of V2-specific monoclonal antibodies from HIV-1-infected individuals. Virology 427:198-207.
76. Nyambi PN, Mbah HA, Burda S, Williams C, Gorny MK, Nadas A, Zolla-Pazner S. 2000. Conserved and exposed epitopes on intact, native, primary human immunodeficiency virus type 1 virions of group M. J Virol 74:7096-107.
77. Pinter A, Honnen WJ, He Y, Gorny MK, Zolla-Pazner S, Kayman SC. 2004. The V1/V2 domain of gp120 is a global regulator of the sensitivity of primary human immunodeficiency virus type 1 isolates to neutralization by antibodies commonly induced upon infection. J Virol 78:5205-15.
78. Gorny MK, Conley AJ, Karwowska S, Buchbinder A, Xu JY, Emini EA, Koenig S, Zolla-Pazner S. 1992. Neutralization of diverse human immunodeficiency virus type 1 variants by an anti-V3 human monoclonal antibody. J Virol 66:7538-42.
79. Gorny MK, Williams C, Volsky B, Revesz K, Wang XH, Burda S, Kimura T, Konings FA, Nadas A, Anyangwe CA, Nyambi P, Krachmarov C, Pinter A, Zolla-Pazner S. 2006. Cross-clade neutralizing activity of human anti-V3 monoclonal antibodies derived from the cells of individuals infected with non-B clades of human immunodeficiency virus type 1. J Virol 80:6865-72.
80. Hioe CE, Wrin T, Seaman MS, Yu X, Wood B, Self S, Williams C, Gorny MK, Zolla-Pazner S. 2010. Anti-V3 monoclonal antibodies display broad neutralizing activities against multiple HIV-1 subtypes. PLoS One 5:e10254.
81. Gigler A, Dorsch S, Hemauer A, Williams C, Kim S, Young NS, Zolla-Pazner S, Wolf H, Gorny MK, Modrow S. 1999. Generation of neutralizing human monoclonal antibodies against parvovirus B19 proteins. J Virol 73:1974-9.

82. Bradley KA, Mogridge J, Mourez M, Collier RJ, Young JA. 2001. Identification of the cellular receptor for anthrax toxin. Nature 414:225-9.
83. Upadhyay C, Feyznezhad R, Yang W, Zhang H, Zolla-Pazner S, Hioe CE. 2018. Alterations of HIV-1 envelope phenotype and antibody-mediated neutralization by signal peptide mutations. PLoS Pathog 14:e1006812.
84. Upadhyay C, Feyznezhad R, Cao L, Chan K-W, Liu K, Yang W, Zhang H, Yolitz J, Arthos J, Nadas A. 2020. Signal peptide of HIV-1 envelope modulates glycosylation impacting exposure of V1V2 and other epitopes. PLoS pathogens 16:e1009185.
85. Rossio JL, Esser MT, Suryanarayana K, Schneider DK, Bess JW, Jr., Vasquez GM, Wiltrout TA, Chertova E, Grimes MK, Sattentau Q, Arthur LO, Henderson LE, Lifson JD. 1998. Inactivation of human immunodeficiency virus type 1 infectivity with preservation of conformational and functional integrity of virion surface proteins. J Virol 72:7992-8001.
86. Altman JB, Liu X, Itri V, Zolla-Pazner S, Powell RLR. 2018. Optimized protocol for detection of native, full-length HIV-1 envelope on the surface of transfected cells. Health Sci Rep 1:e74.
87. Arakelyan A, Fitzgerald W, Margolis L, Grivel JC. 2013. Nanoparticle-based flow virometry for the analysis of individual virions. J Clin Invest 123:3716-27.
88. Arakelyan A, Fitzgerald W, King DF, Rogers P, Cheeseman HM, Grivel JC, Shattock RJ, Margolis L. 2017. Flow virometry analysis of envelope glycoprotein conformations on individual HIV virions. Sci Rep 7:948.
89. Staropoli I, Dufloo J, Ducher A, Commere PH, Sartori-Rupp A, Novault S, Bruel T, Lorin V, Mouquet H, Schwartz O, Casartelli N. 2020. Flow Cytometry Analysis of HIV-1 Env Conformations at the Surface of Infected Cells and Virions: Role of Nef, CD4, and SERINC5. J Virol 94.
90. Julien JP, Cupo A, Sok D, Stanfield RL, Lyumkis D, Deller MC, Klasse PJ, Burton DR, Sanders RW, Moore JP, Ward AB, Wilson IA. 2013. Crystal structure of a soluble cleaved HIV-1 envelope trimer. Science 342:1477-83.
91. Lyumkis D, Julien JP, de Val N, Cupo A, Potter CS, Klasse PJ, Burton DR, Sanders RW, Moore JP, Carragher B, Wilson IA, Ward AB. 2013. Cryo-EM structure of a fully glycosylated soluble cleaved HIV-1 envelope trimer. Science 342:1484-90.
92. Matyas GR, Beck Z, Karasavvas N, Alving CR. 2009. Lipid binding properties of 4E10, 2F5, and WR304 monoclonal antibodies that neutralize HIV-1. Biochim Biophys Acta 1788:660-5.
93. Alam SM, McAdams M, Boren D, Rak M, Scearce RM, Gao F, Camacho ZT, Gewirth D, Kelsoe G, Chen P, Haynes BF. 2007. The role of antibody polyspecificity and lipid reactivity in binding of broadly neutralizing anti-HIV-1 envelope human monoclonal antibodies 2F5 and 4E10 to glycoprotein 41 membrane proximal envelope epitopes. J Immunol 178:4424-35.
94. Falkowska E, Le KM, Ramos A, Doores KJ, Lee JH, Blattner C, Ramirez A, Derking R, van Gils MJ, Liang CH, McBride R, von Bredow B, Shivatare SS, Wu CY, Chan-Hui PY, Liu Y, Feizi T, Zwick MB, Koff WC, Seaman MS, Swiderek K, Moore JP, Evans D, Paulson JC, Wong CH, Ward AB, Wilson IA, Sanders RW, Poignard P, Burton DR. 2014. Broadly neutralizing HIV antibodies define a glycan-

dependent epitope on the prefusion conformation of gp41 on cleaved envelope trimers. Immunity 40:657-68.

95. Moulard M, Hallenberger S, Garten W, Klenk HD. 1999. Processing and routage of HIV glycoproteins by furin to the cell surface. Virus Res 60:55-65.

96. Blattner C, Lee JH, Sliepen K, Derking R, Falkowska E, de la Pena AT, Cupo A, Julien JP, van Gils M, Lee PS, Peng W, Paulson JC, Poignard P, Burton DR, Moore JP, Sanders RW, Wilson IA, Ward AB. 2014. Structural delineation of a quaternary, cleavage-dependent epitope at the gp41-gp120 interface on intact HIV-1 Env trimers. Immunity 40:669-80.

97. Hioe CE, Kumar R, Upadhyay C, Jan M, Fox A, Itri V, Peachman KK, Rao M, Liu L, Lo NC, Tuen M, Jiang X, Kong XP, Zolla-Pazner S. 2018. Modulation of Antibody Responses to the V1V2 and V3 Regions of HIV-1 Envelope by Immune Complex Vaccines. Front Immunol 9:2441.

98. Tang AF, Enyindah-Asonye G, Hioe CE. 2021. Immune Complex Vaccine Strategies to Combat HIV-1 and Other Infectious Diseases. Vaccines (Basel) 9.

99. Zolla-Pazner S, Cohen SS, Boyd D, Kong XP, Seaman M, Nussenzweig M, Klein F, Overbaugh J, Totrov M. 2016. Structure/Function Studies Involving the V3 Region of the HIV-1 Envelope Delineate Multiple Factors That Affect Neutralization Sensitivity. J Virol 90:636-49.

100. Powell RLR, Totrov M, Itri V, Liu X, Fox A, Zolla-Pazner S. 2017. Plasticity and Epitope Exposure of the HIV-1 Envelope Trimer. J Virol doi:10.1128/JVI.00410-17.

101. Sanders RW, Derking R, Cupo A, Julien JP, Yasmeen A, de Val N, Kim HJ, Blattner C, de la Pena AT, Korzun J, Golabek M, de Los Reyes K, Ketas TJ, van Gils MJ, King CR, Wilson IA, Ward AB, Klasse PJ, Moore JP. 2013. A next-generation cleaved, soluble HIV-1 Env trimer, BG505 SOSIP.664 gp140, expresses multiple epitopes for broadly neutralizing but not non-neutralizing antibodies. PLoS Pathog 9:e1003618.

102. Stamatatos L, Wiskerchen M, Cheng-Mayer C. 1998. Effect of major deletions in the V1 and V2 loops of a macrophage-tropic HIV type 1 isolate on viral envelope structure, cell entry, and replication. AIDS Res Hum Retroviruses 14:1129-39.

103. Saunders CJ, McCaffrey RA, Zharkikh I, Kraft Z, Malenbaum SE, Burke B, Cheng-Mayer C, Stamatatos L. 2005. The V1, V2, and V3 regions of the human immunodeficiency virus type 1 envelope differentially affect the viral phenotype in an isolate-dependent manner. J Virol 79:9069-80.

104. Brandenberg OF, Rusert P, Magnus C, Weber J, Boni J, Gunthard HF, Regoes RR, Trkola A. 2014. Partial rescue of V1V2 mutant infectivity by HIV-1 cell-cell transmission supports the domain's exceptional capacity for sequence variation. Retrovirology 11:75.

105. Krachmarov C, Lai Z, Honnen WJ, Salomon A, Gorny MK, Zolla-Pazner S, Robinson J, Pinter A. 2011. Characterization of structural features and diversity of variable-region determinants of related quaternary epitopes recognized by human and rhesus macaque monoclonal antibodies possessing unusually potent neutralizing activities. J Virol 85:10730-40.

106. Robinson JE, Franco K, Elliott DH, Maher MJ, Reyna A, Montefiori DC, Zolla-Pazner S, Gorny MK, Kraft Z, Stamatatos L. 2010. Quaternary epitope specificities

of anti-HIV-1 neutralizing antibodies generated in rhesus macaques infected by the simian/human immunodeficiency virus SHIVSF162P4. J Virol 84:3443-53.

107. Honnen WJ, Krachmarov C, Kayman SC, Gorny MK, Zolla-Pazner S, Pinter A. 2007. Type-specific epitopes targeted by monoclonal antibodies with exceptionally potent neutralizing activities for selected strains of human immunodeficiency virus type 1 map to a common region of the V2 domain of gp120 and differ only at single positions from the clade B consensus sequence. J Virol 81:1424-32.

108. Gorny MK, Stamatatos L, Volsky B, Revesz K, Williams C, Wang XH, Cohen S, Staudinger R, Zolla-Pazner S. 2005. Identification of a new quaternary neutralizing epitope on human immunodeficiency virus type 1 virus particles. J Virol 79:5232-7.

109. Qualls ZM, Choudhary A, Honnen W, Prattipati R, Robinson JE, Pinter A. 2018. Identification of Novel Structural Determinants in MW965 Env That Regulate the Neutralization Phenotype and Conformational Masking Potential of Primary HIV-1 Isolates. J Virol 92.

110. Kulp DW, Steichen JM, Pauthner M, Hu X, Schiffner T, Liguori A, Cottrell CA, Havenar-Daughton C, Ozorowski G, Georgeson E, Kalyuzhniy O, Willis JR, Kubitz M, Adachi Y, Reiss SM, Shin M, de Val N, Ward AB, Crotty S, Burton DR, Schief WR. 2017. Structure-based design of native-like HIV-1 envelope trimers to silence non-neutralizing epitopes and eliminate CD4 binding. Nat Commun 8:1655.

111. Chuang GY, Geng H, Pancera M, Xu K, Cheng C, Acharya P, Chambers M, Druz A, Tsybovsky Y, Wanninger TG, Yang Y, Doria-Rose NA, Georgiev IS, Gorman J, Joyce MG, O'Dell S, Zhou T, McDermott AB, Mascola JR, Kwong PD. 2017. Structure-Based Design of a Soluble Prefusion-Closed HIV-1 Env Trimer with Reduced CD4 Affinity and Improved Immunogenicity. J Virol 91.

112. Kwon YD, Pancera M, Acharya P, Georgiev IS, Crooks ET, Gorman J, Joyce MG, Guttman M, Ma X, Narpala S, Soto C, Terry DS, Yang Y, Zhou T, Ahlsen G, Bailer RT, Chambers M, Chuang GY, Doria-Rose NA, Druz A, Hallen MA, Harned A, Kirys T, Louder MK, O'Dell S, Ofek G, Osawa K, Prabhakaran M, Sastry M, Stewart-Jones GB, Stuckey J, Thomas PV, Tittley T, Williams C, Zhang B, Zhao H, Zhou Z, Donald BR, Lee LK, Zolla-Pazner S, Baxa U, Schon A, Freire E, Shapiro L, Lee KK, Arthos J, Munro JB, Blanchard SC, Mothes W, Binley JM, et al. 2015. Crystal structure, conformational fixation and entry-related interactions of mature ligand-free HIV-1 Env. Nat Struct Mol Biol 22:522-31.

113. Friedrich N, Stiegeler E, Glogl M, Lemmin T, Hansen S, Kadelka C, Wu Y, Ernst P, Maliqi L, Foulkes C, Morin M, Eroglu M, Liechti T, Ivan B, Reinberg T, Schaefer JV, Karakus U, Ursprung S, Mann A, Rusert P, Kouyos RD, Robinson JA, Gunthard HF, Pluckthun A, Trkola A. 2021. Distinct conformations of the HIV-1 V3 loop crown are targetable for broad neutralization. Nat Commun 12:6705.

114. Lai JI, Eszterhas SK, Brooks SA, Guo C, Zolla-Pazner S, Seaman MS, Bailey-Kellogg C, Griswold KE, Ackerman ME. 2020. Induction of cross-reactive HIV-1 specific antibody responses by engineered V1V2 immunogens with reduced conformational plasticity. Vaccine 38:3436-3446.

115. Kubota-Koketsu R, Yunoki M, Okuno Y, Ikuta K. 2021. Virus Neutralization by Human Intravenous Immunoglobulin Against Influenza Virus Subtypes A/H5 and A/H7. Biologics 15:87-94.

116. Kasel JA, Couch RB, Gerin JL, Schulman JL. 1973. Effect of influenza anti-neuraminidase antibody on virus neutralization. Infect Immun 8:130-1.
117. Valenzuela Nieto G, Jara R, Watterson D, Modhiran N, Amarilla AA, Himelreichs J, Khromykh AA, Salinas-Rebolledo C, Pinto T, Cheuquemilla Y, Margolles Y, Lopez Gonzalez Del Rey N, Miranda-Chacon Z, Cuevas A, Berking A, Deride C, Gonzalez-Moraga S, Mancilla H, Maturana D, Langer A, Toledo JP, Muller A, Uberti B, Krall P, Ehrenfeld P, Blesa J, Chana-Cuevas P, Rehren G, Schwefel D, Fernandez LA, Rojas-Fernandez A. 2021. Potent neutralization of clinical isolates of SARS-CoV-2 D614 and G614 variants by a monomeric, sub-nanomolar affinity nanobody. Sci Rep 11:3318.
118. Hu J, Peng P, Wang K, Fang L, Luo FY, Jin AS, Liu BZ, Tang N, Huang AL. 2021. Emerging SARS-CoV-2 variants reduce neutralization sensitivity to convalescent sera and monoclonal antibodies. Cell Mol Immunol 18:1061-1063.
119. Garcia-Beltran WF, Lam EC, St Denis K, Nitido AD, Garcia ZH, Hauser BM, Feldman J, Pavlovic MN, Gregory DJ, Poznansky MC, Sigal A, Schmidt AG, Iafrate AJ, Naranbhai V, Balazs AB. 2021. Multiple SARS-CoV-2 variants escape neutralization by vaccine-induced humoral immunity. Cell 184:2372-2383 e9.
120. Diamond M, Chen R, Xie X, Case J, Zhang X, VanBlargan L, Liu Y, Liu J, Errico J, Winkler E, Suryadevara N, Tahan S, Turner J, Kim W, Schmitz A, Thapa M, Wang D, Boon A, Pinto D, Presti R, O'Halloran J, Kim A, Deepak P, Fremont D, Corti D, Virgin H, Crowe J, Droit L, Ellebedy A, Shi PY, Gilchuk P. 2021. SARS-CoV-2 variants show resistance to neutralization by many monoclonal and serum-derived polyclonal antibodies. Res Sq doi:10.21203/rs.3.rs-228079/v1.
121. Cheng CC, Platen L, Christa C, Tellenbach M, Kappler V, Bester R, Liao BH, Holzmann-Littig C, Werz M, Schonhals E, Platen E, Eggerer P, Treguer L, Kuchle C, Schmaderer C, Heemann U, Renders L, Protzer U, Braunisch MC. 2022. Improved SARS-CoV-2 Neutralization of Delta and Omicron BA.1 Variants of Concern after Fourth Vaccination in Hemodialysis Patients. Vaccines (Basel) 10.
122. Chertova E, Bess JW, Jr., Crise BJ, Sowder IR, Schaden TM, Hilburn JM, Hoxie JA, Benveniste RE, Lifson JD, Henderson LE, Arthur LO. 2002. Envelope glycoprotein incorporation, not shedding of surface envelope glycoprotein (gp120/SU), Is the primary determinant of SU content of purified human immunodeficiency virus type 1 and simian immunodeficiency virus. J Virol 76:5315-25.
123. Zhu P, Liu J, Bess J, Jr., Chertova E, Lifson JD, Grise H, Ofek GA, Taylor KA, Roux KH. 2006. Distribution and three-dimensional structure of AIDS virus envelope spikes. Nature 441:847-52.
124. Poignard P, Moulard M, Golez E, Vivona V, Franti M, Venturini S, Wang M, Parren PW, Burton DR. 2003. Heterogeneity of envelope molecules expressed on primary human immunodeficiency virus type 1 particles as probed by the binding of neutralizing and nonneutralizing antibodies. J Virol 77:353-65.
125. Brandenberg OF, Magnus C, Regoes RR, Trkola A. 2015. The HIV-1 Entry Process: A Stoichiometric View. Trends Microbiol 23:763-774.
126. Yang X, Kurteva S, Ren X, Lee S, Sodroski J. 2006. Subunit stoichiometry of human immunodeficiency virus type 1 envelope glycoprotein trimers during virus entry into host cells. J Virol 80:4388-95.

127. Yang X, Kurteva S, Ren X, Lee S, Sodroski J. 2005. Stoichiometry of envelope glycoprotein trimers in the entry of human immunodeficiency virus type 1. J Virol 79:12132-47.
128. Mangala Prasad V, Leaman DP, Lovendahl KN, Croft JT, Benhaim MA, Hodge EA, Zwick MB, Lee KK. 2022. Cryo-ET of Env on intact HIV virions reveals structural variation and positioning on the Gag lattice. Cell doi:10.1016/j.cell.2022.01.013.
129. Li L, Wang XH, Williams C, Volsky B, Steczko O, Seaman MS, Luthra K, Nyambi P, Nadas A, Giudicelli V, Lefranc MP, Zolla-Pazner S, Gorny MK. 2015. A broad range of mutations in HIV-1 neutralizing human monoclonal antibodies specific for V2, V3, and the CD4 binding site. Mol Immunol 66:364-374.
130. Moore JP, Sattentau QJ, Yoshiyama H, Thali M, Charles M, Sullivan N, Poon SW, Fung MS, Traincard F, Pinkus M, et al. 1993. Probing the structure of the V2 domain of human immunodeficiency virus type 1 surface glycoprotein gp120 with a panel of eight monoclonal antibodies: human immune response to the V1 and V2 domains. J Virol 67:6136-51.
131. McKeating JA, Shotton C, Cordell J, Graham S, Balfe P, Sullivan N, Charles M, Page M, Bolmstedt A, Olofsson S, et al. 1993. Characterization of neutralizing monoclonal antibodies to linear and conformation-dependent epitopes within the first and second variable domains of human immunodeficiency virus type 1 gp120. J Virol 67:4932-44.
132. Tuen M, Bimela JS, Banin AN, Ding S, Harkins GW, Weiss S, Itri V, Durham AR, Porcella SF, Soni S, Mayr L, Meli J, Torimiro JN, Tongo M, Wang X, Kong XP, Nadas A, Kaufmann DE, Brumme ZL, Nanfack AJ, Quinn TC, Zolla-Pazner S, Redd AD, Finzi A, Gorny MK, Nyambi PN, Duerr R. 2019. Immune Correlates of Disease Progression in Linked HIV-1 Infection. Front Immunol 10:1062.
133. Liu L, Li L, Nanfack A, Mayr LM, Soni S, Kohutnicki A, Agyingi L, Wang XH, Tuen M, Shao Y, Totrov M, Zolla-Pazner S, Kong XP, Duerr R, Gorny MK. 2019. Anti-V2 antibody deficiency in individuals infected with HIV-1 in Cameroon. Virology 529:57-64.

Table 1. Binding specificity of the monoclonal antibodies (mAbs) used in the study.

Antibody name	Epitope/ binding site	Structural preference
697 830A 2158	gp120 V1V2 (V2i)	Conformational
CH58 CH59	gp120 V1V2 (V2p)	Linear
PG9 PG16 PGT145 PGDM1400	gp120 V1V2 (V2q)	Conformational
2219 2557	gp120 V3	Linear
NIH45-46 VRC01 b12 3BNC117	gp120 CD4 binding site (CD4BS)	Conformational
PGT151	gp120-gp41 interface	
VRC34	gp41 fusion peptide/gp120 glycan	
4E10 2F5	gp41 MPER	Linear
3685	anti-parvovirus	Non-binding

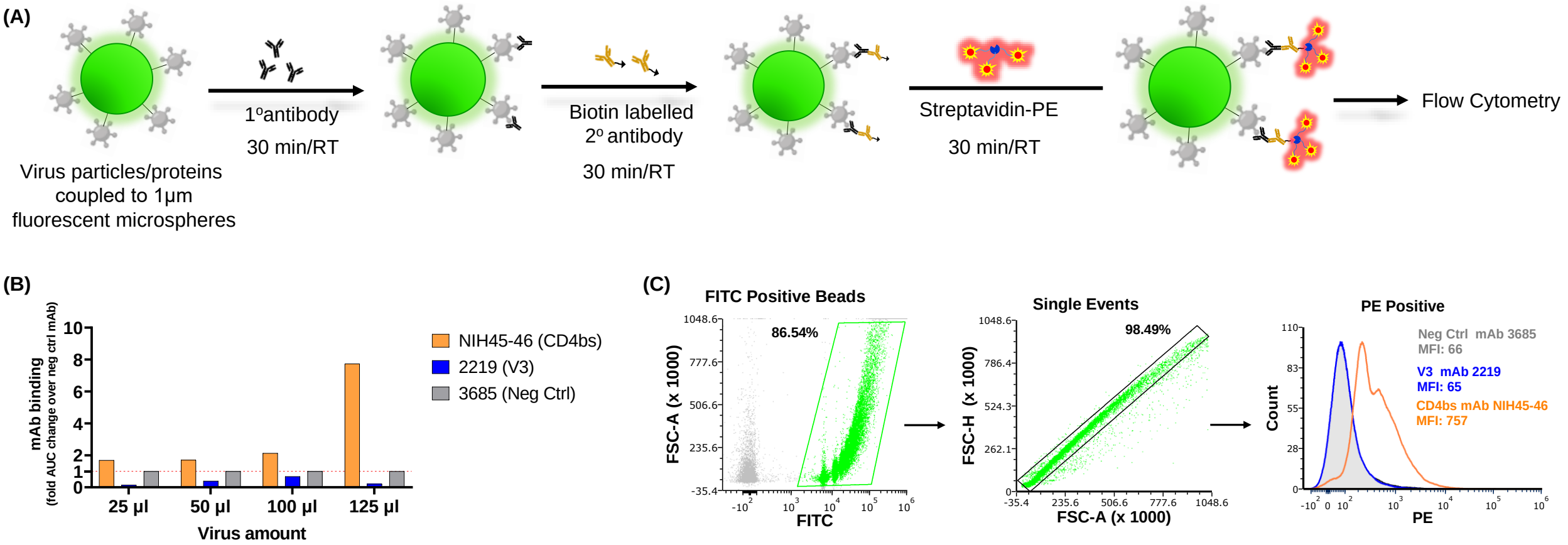

Figure. 1. Virus-binding assay for detection of antibody binding to Env expressed on virions. (A) Schematic of the assay; (B) Optimization of virus amount to be coupled to the microspheres; (C) Representative dot plots and histogram showing the gating strategy for analysis of antibodies binding to virus particle by flow cytometry. The mAbs were tested at following concentrations: NIH45-46 at 5 µg/ml; 2219 and 3685 at 50 µg/ml. 1°, primary; 2° secondary.

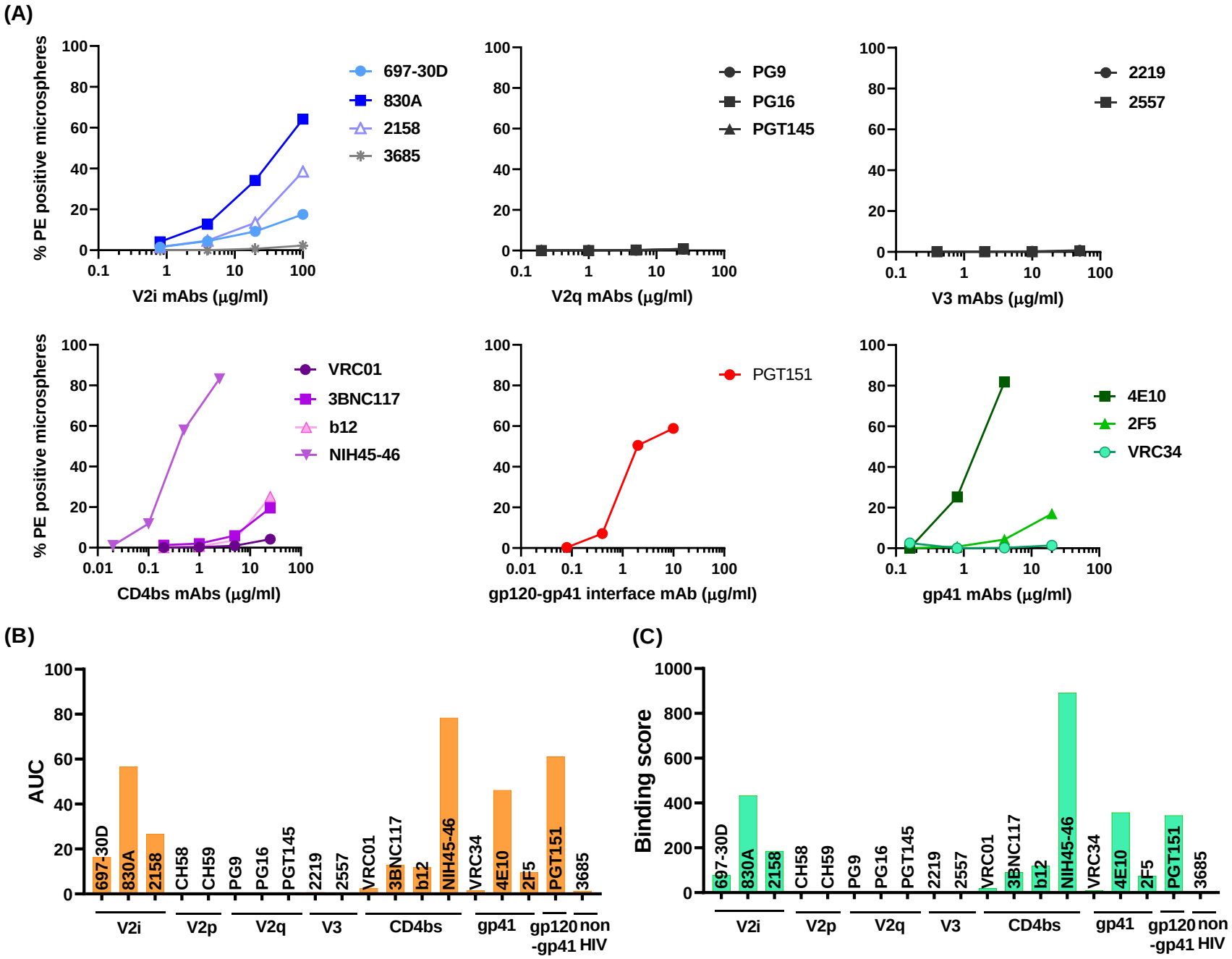

Figure 2. Binding of mAbs to REJO Env on virions. (A) Microspheres coupled to REJO virus were reacted with serially diluted mAbs targeting different Env epitopes. (B) Area under the curve (AUC) were calculated from the curves in A and plotted. (C) Binding score (BS) was calculated by multiplying the percent gated PE positive beads with geometric mean fluorescent intensity (MFI) of each mAb tested at a single dilution. This value was divided by hundred and is plotted. Virus coupled microspheres stained with biotin and PE alone were used to set the background BS and subtracted. X, not tested.

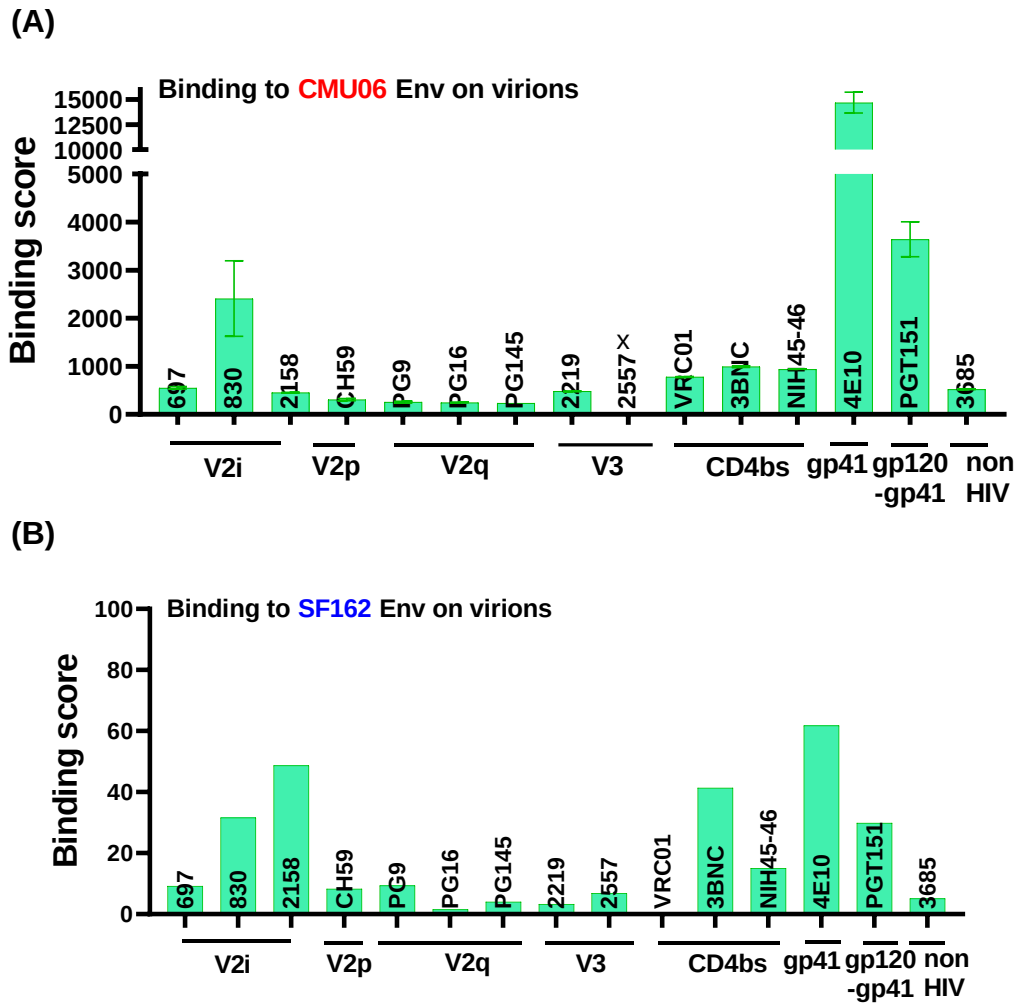

Figure 3. Binding of mAbs to Env on virions. Microspheres coupled to (A) CMU06 and (B) SF162 viruses were incubated with mAbs targeting different Env epitopes. Binding scores (BS) were calculated by multiplying the percent gated PE positive beads with the geometric mean fluorescence intensity (MFI) of each mAb tested at the single dilution. This value was divided by one hundred and is plotted. Virus coupled microspheres stained with biotin and PE alone were used to set the background BS and subtracted. The mAbs were tested at following concentrations: 697, 830A, 2158, 3685 at 100 µg/ml; 2219, 2557 at 50 µg/ml; PG9, PG16, PGT145, CH59, VRC01, 3BNC117 at 25 µg/ml; 4E10 at 20 µg/ml; PGT151 at 10 µg/ml; NIH45-46 at 5 µg/ml. X, not tested.

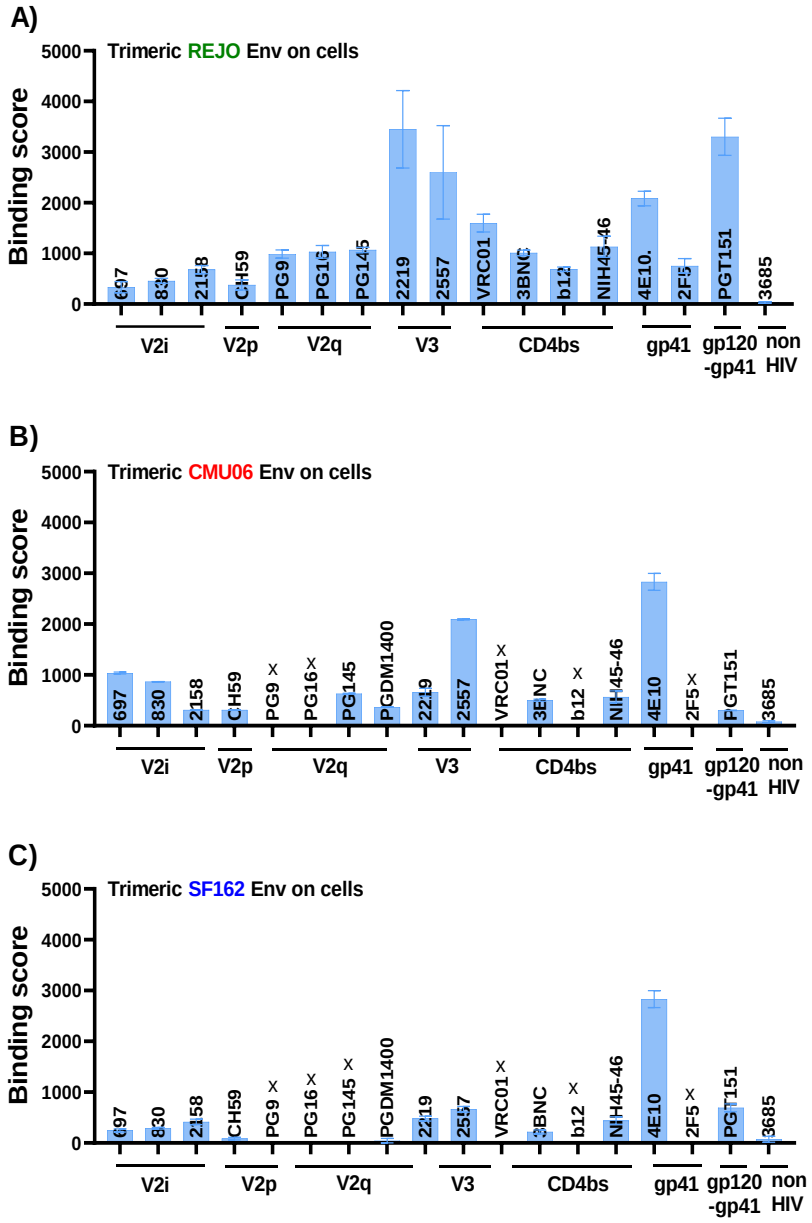

Figure 4. Binding of mAbs to trimeric Env expressed on cell surface. (A) 293T cells were transiently transfected with plasmid encoding for full length gp160. Cells were analyzed for binding of different mAbs 24-hours post-transfection. Binding scores (BS) were calculated by multiplying the percent gated PE positive cells with geometric mean fluorescence intensity (MFI) of each mAb tested at the single dilution. This value was divided by one hundred and is plotted. Transfected cells stained with biotin and PE alone were used to set the background BS and subtracted. X, not tested. The mAbs were tested at following concentrations: 697, 830A, 2158, 3685 at 100 µg/ml; 2219, 2557 at 50 µg/ml; PG9, PG16, PGT145, PGDM1400, CH59, VRC01, 3BNC117, b12 at 25 µg/ml; 4E10, 2F5 at 20 µg/ml; PGT151 at 10 µg/ml; NIH45-46 at 5 µg/ml. X, not tested.

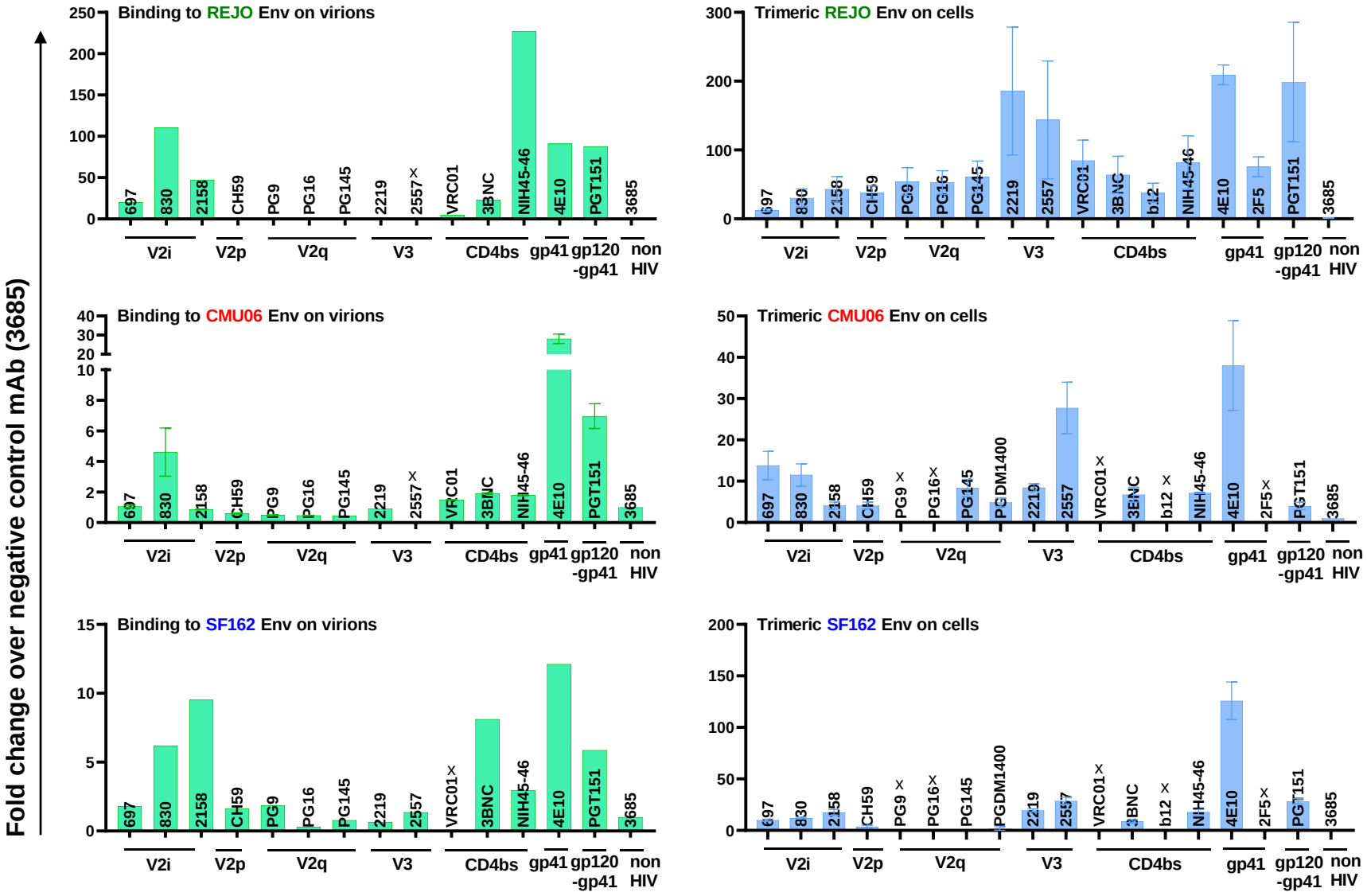

Figure 5. Comparison of binding of mAbs to Env on virions and cell surface. Binding data in figures 2, 3 and 4 was normalized and shown as fold change over negative control mAb 3685. X, not tested.

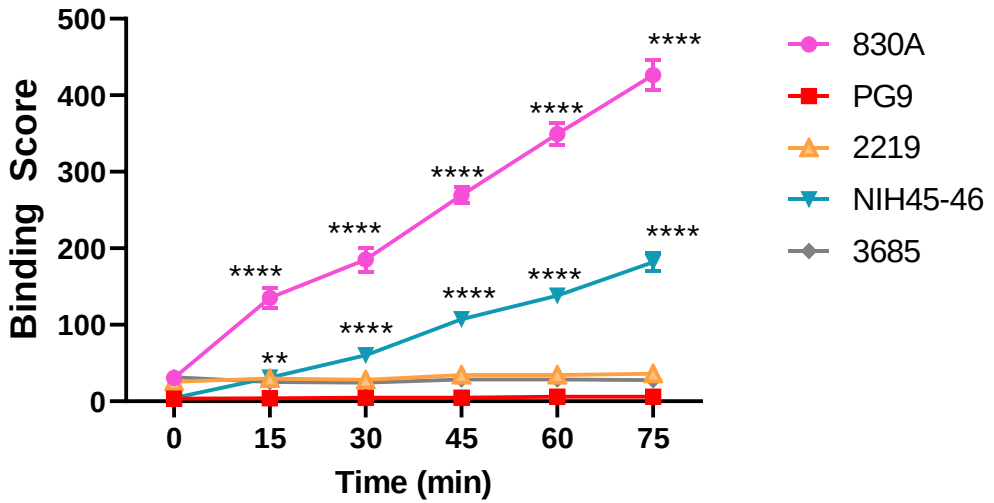

Figure 6. Time-dependent increase of Env binding. Microspheres coupled to REJO virus particles were treated with mAbs at 37°C for various time from 0 to 75 min. Binding was detected as in Figure 2 and binding scores (BS) are shown. The mAbs were tested at following concentrations: 830A, 3685 at 100 µg/ml; 2219 at 50 µg/ml; PG9 at 25 µg/ml; NIH45-46 at 2.5 µg/ml. ****, p= <0.0001; **, p= 0.0026 vs t = 0 min by ANOVA.

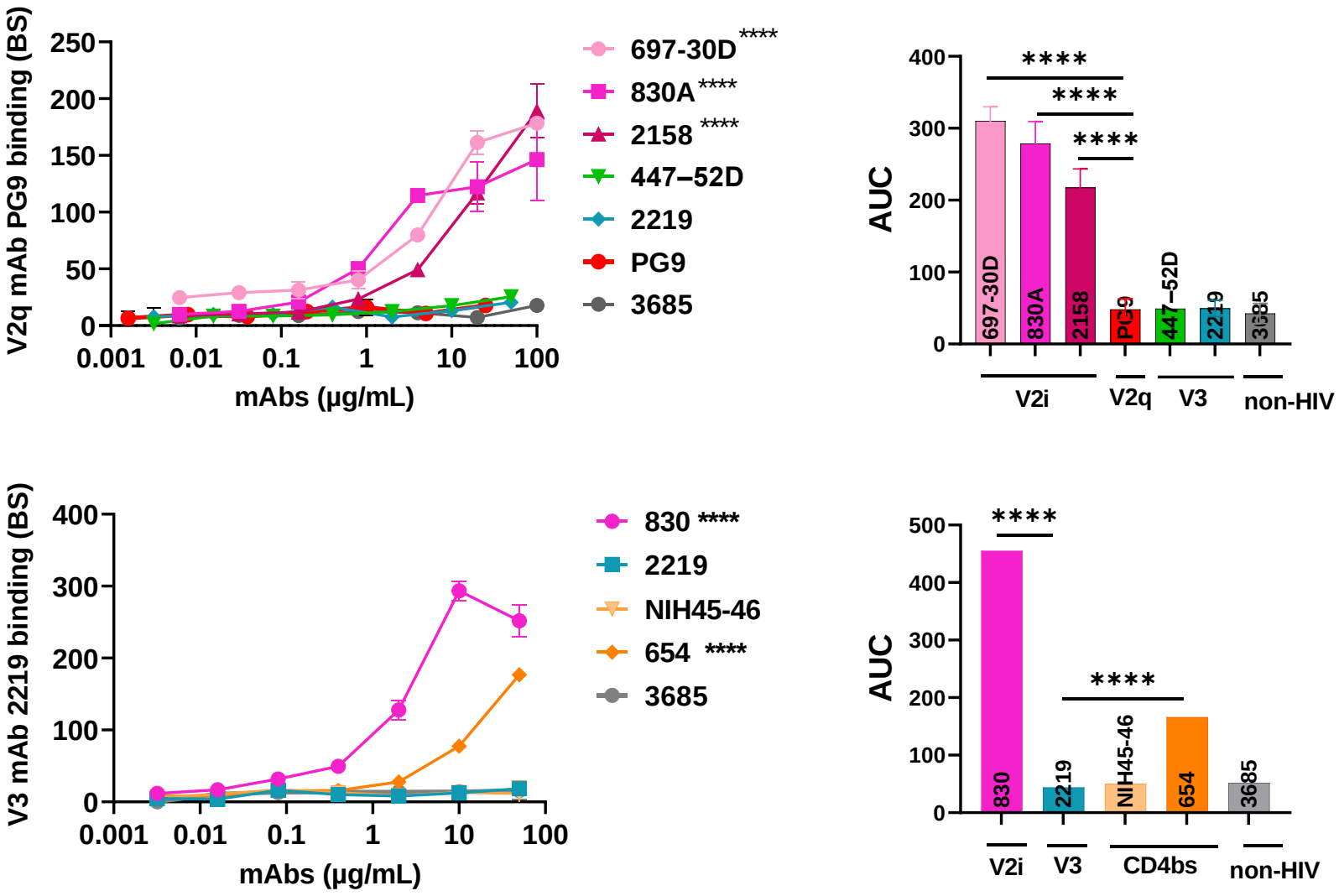

Figure 7. Changes in reactivity of PG9 and 2219 mAbs. Microspheres coupled with REJO virus were incubated with titrated amounts of antibodies followed by biotinylated V2q mAb PG9 (25 µg/ml) or biotinylated V3 mAb 2219 (50 µg/ml). Binding was detected with streptavidin-PE. **** p< 0.0001 by ANOVA.

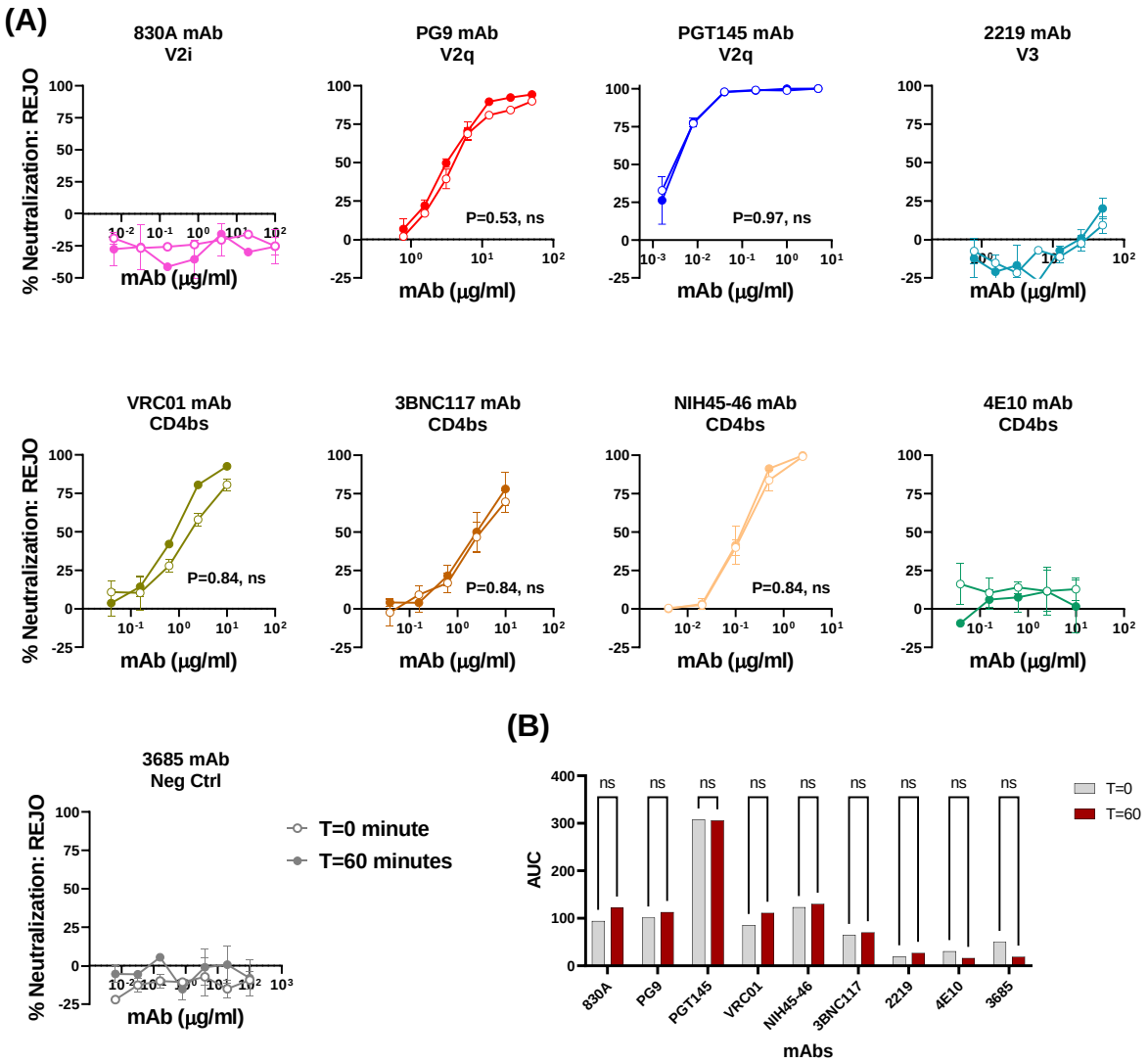

Figure 8. Neutralization of REJO virus. Virus neutralization was measured after REJO was incubated with serially diluted mAbs for the designated period of time at 37°C prior to the addition of TZM-bl target cells. Virus infectivity was assessed 48 h later based on β-galactosidase activity. (A) Neutralization curves are shown. Means and standard errors calculated from two different experiments (each in duplicate) are shown. Statistical analyses were performed on the neutralization curves reaching ≥50%. Comparison is made between neutralization curves at T = 0 vs T = 60 minutes. P= ns, not significant by nonparametric Mann-Whitney t-test. (B) Area under the neutralization curves were calculated and plotted as bar graph. Statistical analysis was performed on AUC graph by ANOVA (P = 0.99; ns, not significant).

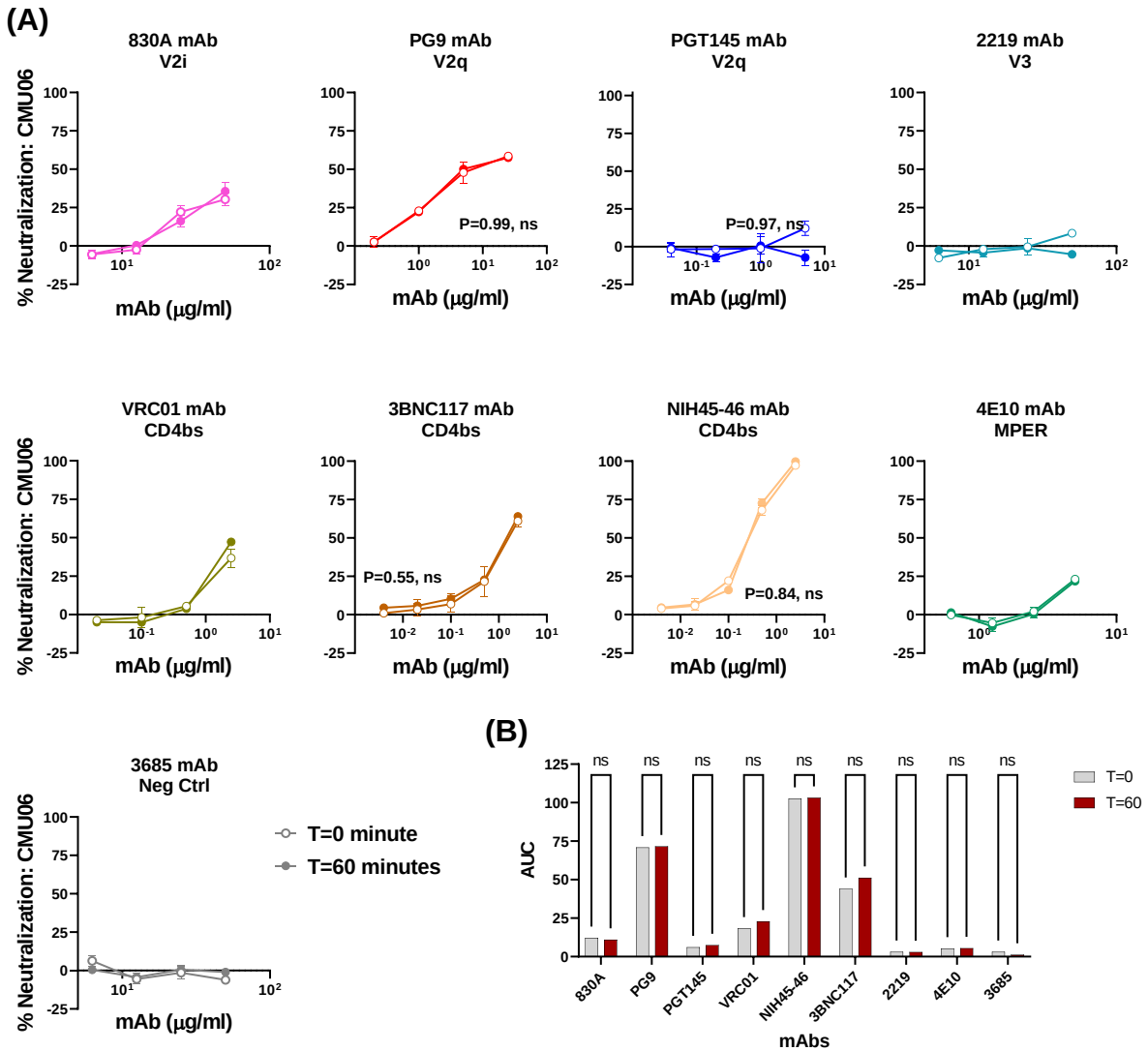

Figure 9. Neutralization of CMU06 virus. Virus neutralization was measured after CMU06 was incubated with serially diluted mAbs for the designated period of time at 37°C prior to the addition of TZM-bl target cells. Virus infectivity was assessed 48 h later based on β-galactosidase activity. (A) Neutralization curves are shown. Means and standard errors calculated from two different experiments (each in duplicate) are shown. Statistical analyses were performed on the neutralization curves reaching ≥50%. Comparison is made between neutralization curves at T = 0 vs T = 60 minutes. P= ns, not significant by nonparametric Mann-Whitney t-test. (B) Area under the neutralization curves were calculated and plotted as bar graph. Statistical analysis was performed on AUC graph by ANOVA (P = 0.99; ns, not significant)

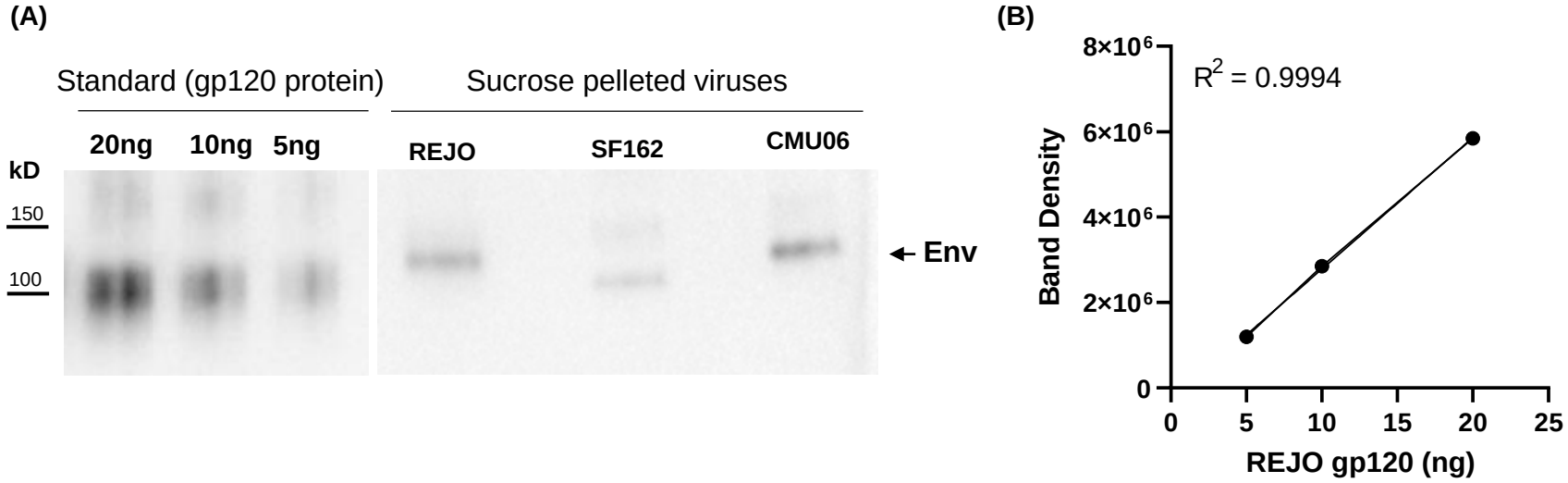

Supplementary Figure 1. Measurement of Env in virus preparations by Western blot. (A) Viruses produced in 293T cells, were concentrated (20X) by sucrose pelleting. 4 µl of each 20X concentrated virus particles were lysed and analyzed by SDS-PAGE (4–20%) and Western blot. An anti-gp120 MAb cocktail (V3: 391/95-D, 694/98-D, 2219, 2558; C2: 847-D, 1006-30D; C5: 450-D, 670-D) was used to quantitate the levels of Env associated with virions. REJO gp120 protein loaded at different concentrations was used as standard. The band density of REJO gp120 protein was used to generate the linear curve (B) and to calculate the amount of Env in each virus preparation.